

Assessing seismic soil liquefaction susceptibility and hazard zonation in Bihar, India: a comparative study of deterministic methods

Ishwar Chandra Thakur^{1*} and Lal Bahadur Roy²

Research Scholar, Department of Civil Engineering, NIT Patna, Bihar, India¹

Professor, Department of Civil Engineering, NIT Patna, Bihar, India²

Received: 13-August-2023; Revised: 21-April-2024; Accepted: 23-April-2024

©2024 Ishwar Chandra Thakur and Lal Bahadur Roy. This is an open access article distributed under the Creative Commons Attribution (CC BY) License, which permits unrestricted use, distribution, and reproduction in any medium, provided the original work is properly cited.

Abstract

Bihar is a heavily populated state in India. It is experiencing a rapid increase in construction activities due to industrial expansion. The state is known for its high seismic activity, having experienced several earthquakes in the past, including the devastating 1934 earthquake and the most recent in 2015. The alluvial deposits in the Indo-Gangetic plain of Bihar caused substantial seismic soil liquefaction. Overpopulation and poor construction techniques have caused extensive damage to property and life. This study aims to provide an assessment of the seismic soil liquefaction susceptibility of Bihar with varying earthquake magnitudes (M_w) of 6.0, 6.5, 7.0, and 7.5. In the present study, two deterministic methods given by Tokimatsu and Yoshimi (1983) and IS 1893 (Part 1): (2016) have been used, and their results have been compared. Also, the study intends to produce a hazard zonation map of Bihar. The study shows that the liquefaction susceptibility of soil is significantly influenced by the depth of soil below ground level, M_w , standard penetration test (SPT) N-value, and fines content (FC). The hazard zonation maps reveal a high vulnerability of northern districts like Sitamarhi, Madhubani, and Supaul at $M_w = 6.0$. At $M_w = 7.5$, almost the entire state is prone to soil liquefaction. This emphasizes the importance of investigation and highlights the need for careful engineering practices to mitigate liquefaction hazards in Bihar.

Keywords

Standard penetration test blow count, Fines content, Hazard zonation map, Vulnerability, Liquefaction.

1. Introduction

Demographically, Bihar is the densest state in India. As per the 2011 census, the population density of Bihar was 1106, whereas the national average density was 382 persons per square kilometer [1]. Also, the state has over 73% flood-affected areas and is completely landlocked with alluvium strata. The state is more vulnerable to several natural and man-made threats because of its geographical and topographical conditions. Floods, earthquakes, droughts, fire outbreaks, and cyclones are among the many severe disasters that have had an impact on the state in the past [2]. Singh and Pandey [3] found that the northern Bihar plains are drained by many rivers, which yields sediment deposits. IS 1893 (part 1): 2016 [4] divided the plains of Bihar into three seismic zones according to the increasing order of severity, namely zones III, IV, and V. The state has a history of moderate-to-severe earthquakes.

Rajendran et al. [5] stated that there was a tremendous amount of soil liquefaction in Bihar and Nepal during the great earthquake of 1934. The energy of this earthquake was greater than 1022 ergs, which can produce fractures in a solid rock plate dimension greater than 150 km \times 100 km and a thickness of 10 km [6]. It was very devastating due to differences in quality and the type of construction. Maximum shaking intensity was "X" on the Modified Mercalli Intensity (MMI) scale [7, 8].

The Alpid belt of the Himalayas, adjacent to Bihar in the north, is one of the most active intercontinental seismic zones in the world [9]. Sukhija et al. [10], in their palaeoliquefaction study, found that the area is seismically active and meizoseismal. Singh et al. [11] found that Bihar is the worst vulnerable to earthquakes due to the penetration of subsurface fault lines of the Himalayan tectonic plate into the Gangetic plains. The Indo-Gangetic Plains, situated between the Himalayan Mountain ranges and peninsular India, are regarded as a place of major

*Author for correspondence

concern because of their deep sediments and proximity to the Himalayan collision zone, India's seismically most active zone [12]. Central thrust and the West Patna subsurface fault are the reasons for the contribution of maximum PGA [13, 14]. Shams et al. [15], in their study, found that the Kishanganj district of Bihar is vulnerable to seismic hazards due to its high PGA value.

Dey [16], in an investigation, found that the area adjacent to the Bihar-Nepal border is vulnerable to the great magnitude of the earthquake and has evidence of the destruction of many lives. A reconnaissance study by Rai et al. [17] reveals the earthquake vulnerability of Bihar due to its poor construction techniques and high population density. Sinha [18, 19] also reported that poor construction practices and low maintenance of the buildings in Patna, the capital of Bihar, are the causes of large-scale loss of life and property during earthquakes. Factors that make cities in Bihar most hazardous to earthquake tremors and, consequently, to liquefaction include rising demographic pressure, worsening environmental conditions, poverty, a low standard of living, urbanization without a plan in regions with limited lanes, serious traffic congestion issues, and a lack of awareness. Even a modest earthquake that struck the state capital of Patna would cause thousands of structures to collapse and lakhs of people to lose their lives. Inadequately designed homes, buildings, and other structures could be destroyed by an earthquake with a magnitude greater than eight [20, 21]. Congestion, overpopulation, poor house planning, and construction are the primary causes of heavy damage and deaths during earthquakes [22–24]. The primary influencing factors of seismic soil liquefaction are M_w , duration, epicentral distance, particle size, fines content (FC), grain composition, drainage condition, groundwater table, degree of consolidation, relative density, depth of sand layer, and thickness of the sand layer [25–29].

Gautam et al. [30] studied the soil of Kathmandu city, which is adjacent to Bihar, after the 2015 earthquake in Gorkha, Nepal. Soil liquefaction can result in several destructive consequences, such as the emergence of sand boils. This phenomenon occurs during intense earthquakes with multiple cycles of shaking, where the high pressure causes liquefied sand and excessive water to erupt at the ground surface. Additionally, it can lead to foundation failure, unstable terrain that collapses, and sudden land subsidence. Buildings constructed on slopes and

soft ground are susceptible to collapse due to elevation, depression, tilting, or shaking of the earth. However, various ground improvement methods can be used as mitigation techniques against soil liquefaction [31–33].

The soil liquefaction potential indicates the level of vulnerability of the soil to liquefy under the influence of dynamic loads. The measurement of liquefaction potential involves comparing the cyclic resistance ratio (CRR) to the cyclic stress ratio (CSR) produced by an earthquake of a particular magnitude. CRR represents the ability of the soil layer at a given depth, with specific properties, to withstand the cyclic stress that triggers liquefaction. On the other hand, CSR reflects the seismic force exerted on the soil layer during an earthquake incident. After estimating the CRR and CSR values, the factor of safety against liquefaction (FS_L) is computed from Equation 1.

$$FS_L = \frac{CRR}{CSR} \quad (1)$$

This value determines the extent of risk associated with liquefaction and evaluates the level of soil susceptibility during an earthquake incident. Cetin et al. [34] categorized the soil based on its FS_L values. Soil with an FS_L greater than 1.3 is classified as non-liquefiable, whereas soil with an FS_L between 1.1 and 1.3 is regarded as marginally liquefiable, and soils with FS_L values lower than 1.1 are liquefiable. To safeguard against catastrophic failure, the Tokimatsu and Yoshimi (1983) method suggests using an FS_L value higher than 1.5 for normalized standard penetration test (SPT) N-value (N_1) ≤ 10 and 1.3 or less for medium to dense sand [35]. IS 1893 (part 1): 2016 suggests $FS_L > 1.0$ to safeguard against liquefaction. Soil is assumed to liquefy below this value. For conservative ground motion, the permanent deformation will be small in the case of $FS_L \geq 1.2$ [4].

The present study focused on Bihar, which is a landlocked state located in the northern part of India, with coordinates ranging from 24°20'10"N to 27°31'15"N latitude and 83°19'50"E to 88°17'40"E longitude. It shares borders with Jharkhand to the south, Nepal to the north, West Bengal to the east, and Uttar Pradesh to the west. The state is seismically active and is classified into three seismic zones based on the intensity of earthquakes in the region. Seismic Zone V in the northern parts of Bihar is the most active and prone to earthquakes of the highest intensity, while Seismic Zone IV in the central parts and Seismic Zone III in the southern parts are less

active but still vulnerable. The state is situated in the Himalayan foothills and the Ganga basin, which have a complex geological history and a varied geological composition. Bihar has a significant number of sedimentary rocks, such as shale and sandstone, which are known to be relatively weak and can be easily eroded or weathered. The river Ganga flows in an east-west direction, dividing the state into two unequal parts, and its tributaries on both sides of the river cover the entire plains of the state. These hydrological features make the region highly vulnerable to flooding and waterlogging, while the geotechnical characteristics of the state, including

alluvial soil and weak rocks, make it prone to soil liquefaction, landslides, and soil settlement during earthquakes. The water table fluctuates throughout the year. It reaches its maximum during the rainy season and its minimum in the summer. In Figure 1, borehole locations are distinguished by unique station names in alphabetical order, corresponding to the districts within seismic zones. Specifically, stations L01 to L09 pertain to districts within seismic zone III, stations L10 to L31 relate to districts within seismic zone IV, and stations L32 to L33 are associated with districts within seismic zone V.

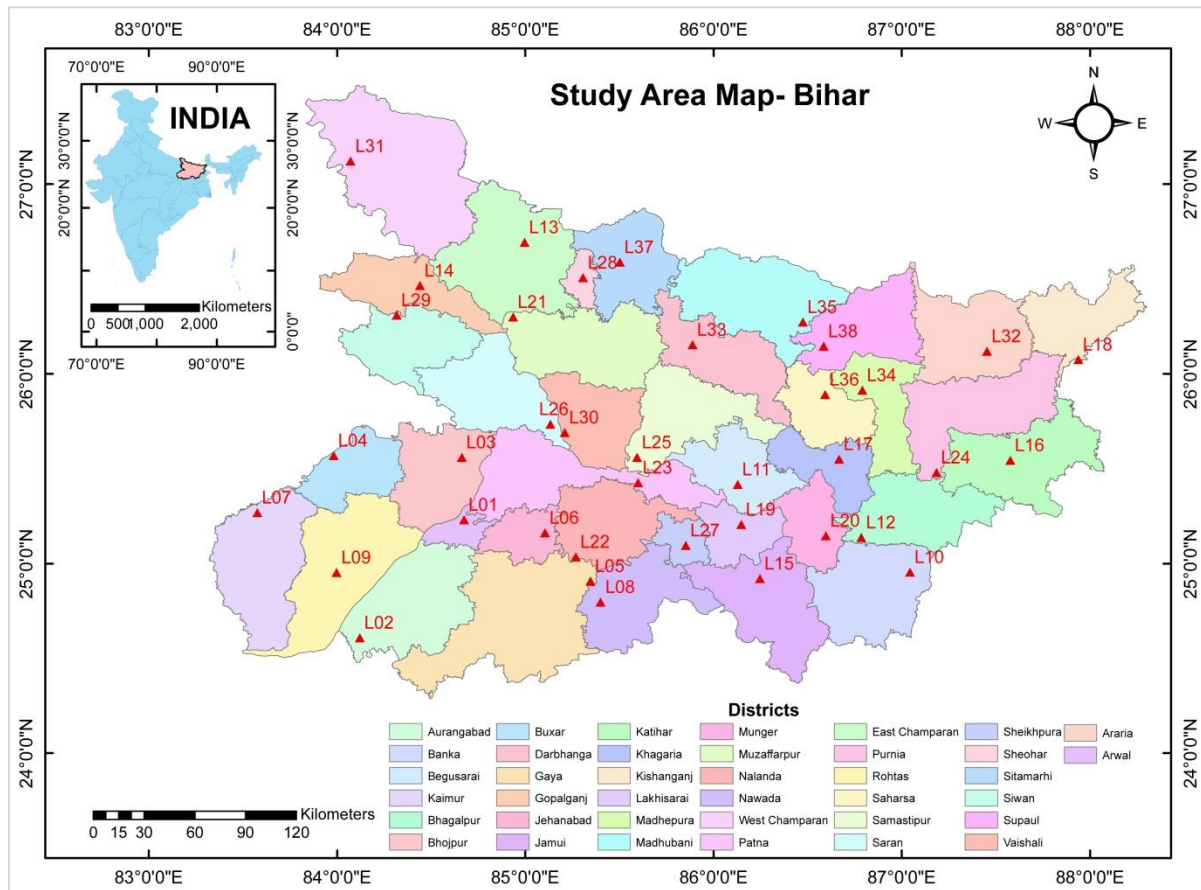


Figure 1 Study area map showing the location of borehole stations (L01 to L38)

In this research, comprehensive geotechnical data has been diligently gathered from a diverse range of reputable sources. All of these have contributed valuable information to the dataset. These sources encompass laboratory reports at NIT Patna and soil investigation agencies associated with the important infrastructure projects of the Government of Bihar. The rotary method of boring was used, and the standard testing procedure was adopted following IS

2131-1981. The collected data consists of several key parameters, including depth, SPT N-value, bulk density (γ_{Bulk}), FC, water content, water table levels at the time of testing, visual descriptions of soil characteristics, and the Bureau of Indian Standard (BIS) soil classification. The scope of the data collection effort covers all 38 districts of Bihar, ensuring a broad representation of soil profiles across the region. To facilitate spatial analysis and mapping,

latitude and longitude coordinates have also been collected for each borehole location. A typical soil profile from borehole stations L13 and L27 has been presented in *Tables 1* and *2*, respectively. The color log displays the layer and extent of the borehole along with the type of soil. The deterministic method discussed in section 3 utilizes soil properties, such as

the SPT N-value, γ_{Bulk} , and FC, along with the stress parameters of the soil. The stress for each layer of soil, including the total vertical stress (σ_{vo}) and effective stress (σ'_{vo}), is presented here. Collectively, these parameters show the in-situ soil condition and its stability.

Table 1 Typical soil profile for a borehole (L13) in East Champaran district of Bihar

Extent of borehole (m)		Visual description of soil with BIS classification	Log	N-Value	γ_{Bulk} (kN/m ³)	FC %	σ_{vo} (kN/m ²)	σ'_{vo} (kN/m ²)
From	To							
0	1.5	Medium dense, brownish grey silty micaceous fine to medium sand, SM		8	17.27	17.00	25.90	11.18
1.5	3.0	Medium dense, brownish grey silty micaceous fine to medium sand, SM		11	17.27	15.00	51.80	22.37
3.0	4.5	Medium dense, brownish grey silty micaceous fine to medium sand, SM		7	17.27	14.00	77.70	33.55
4.5	6.0	Medium dense, brownish grey silty micaceous fine to medium sand, SM		13	17.66	18.00	105.95	47.09
6.0	7.5	Medium dense, brownish grey silty micaceous fine to medium sand, SM		13	17.66	18.00	132.44	58.86
7.5	9.0	Medium dense, brownish grey silty micaceous fine to medium sand, SM		16	17.66	15.00	158.92	70.63
9.0	10.5	Medium dense, brownish grey silty micaceous fine to medium sand, SM		23	17.66	15.00	185.41	82.40
10.5	12.0	Medium dense, brownish grey silty micaceous fine to medium sand, SM		24	18.15	18.00	217.78	100.06
12.0	13.5	Medium dense, brownish grey silty micaceous fine to medium sand, SM		12	18.15	18.00	245.00	112.57
13.5	15.0	Medium dense, brownish grey silty micaceous fine to medium sand, SM		17	18.15	20.00	272.23	125.08
15.0	16.5	Medium dense, brownish grey silty micaceous fine to medium sand, SM		30	18.15	20.00	299.45	137.59
16.5	18.0	Medium dense, brownish grey silty micaceous fine to medium sand, SM		26	18.15	21.00	326.67	150.09
18.0	20.5	Medium dense, brownish grey silty micaceous fine to medium sand, SM		28	18.15	21.00	372.04	170.94
20.5	25.0	Medium dense, brownish grey silty micaceous fine to medium sand, SM		28	18.15	20.00	453.71	208.46
25.0	30.0	Medium dense, brownish grey silty micaceous fine to medium sand, SM		30	18.15	18.00	544.46	250.16

Table 2 Typical soil profile for a borehole (L27) in Sheikhpura district of Bihar

Extent of borehole (m)		Visual description of soil with BIS classification	Log	N-Value	γ_{Bulk} (kN/m ³)	FC %	σ_{vo} (kN/m ²)	σ'_{vo} (kN/m ²)
From	To							
0	1.5	Greyish silty clay, CI		6	19.23	91.50	28.84	14.72
1.5	3.0	Greyish silty clay, CI		8	19.42	91.50	58.27	29.43
3.0	4.5	Greyish silty clay, CI		11	19.62	91.50	88.29	44.15
4.5	6.0	Reddish silty clay, CL		14	19.72	92.60	118.31	58.86
6.0	7.5	Reddish silty clay, CL		17	19.72	92.60	147.89	73.58
7.5	9.0	Reddish silty clay, CL		20	19.82	92.60	178.35	88.29
9.0	10.5	Reddish silty clay, CL		25	19.82	91.90	208.07	103.01
10.5	12.0	Yellowish silty clay, CI		31	19.91	91.90	238.97	117.72
12.0	13.5	Yellowish silty clay, CI		35	19.91	91.90	268.84	132.44
13.5	15.0	Yellowish silty clay, CI		38	20.11	91.20	301.66	147.15

The objective of this study is to provide valuable insights into the geotechnical characteristics of the soils in Bihar, particularly concerning their susceptibility to liquefaction during seismic events. This information can be of immense significance for various engineering and infrastructure projects in the region, helping to enhance safety and stability considerations. By utilizing advanced data analysis techniques and geospatial tools, meaningful correlations and patterns have been drawn from this extensive dataset. The outcome of this research contributes to a better understanding of the geotechnical conditions in Bihar and fosters informed decision-making for future construction and development activities in the region. The following segment of this paper outlines the literature review in section 2. In section 3, the methodology employed for deterministic approaches in determining the FS_L against liquefaction is expounded. Moving forward, section 4 presents the findings, while a thorough discussion of these findings, including their limitations, is presented in section 5. Finally, the paper concludes with section 6, encapsulating the conclusions drawn and outlining potential future directions for this research endeavour.

2.Literature review

Several researchers have made significant contributions to the assessment of soil liquefaction potential. Seed and Idriss [36] devised a technique to evaluate the liquefaction potential of soil. The study identifies factors affecting sand liquefaction during earthquakes and proposes a “simplified procedure” for assessing liquefaction potential. After more than two decades of popularity, the method was modified by Youd and Idriss [37] with 20 experts in 1996. Based on the above, the Indian code of practice IS 1893 (Part 1): 2016 [4] standardized the simplified procedure for the evaluation of liquefaction potential in the country.

Thakur and Roy [29] analyzed liquefaction potential in Bihar using SPT field data from different seismic zones of Bihar. They found the simplified procedure as an effective technique for their study in Bihar. They concluded that the fines content, water table, and SPT N-values have a significant impact on the liquefaction susceptibility of soil. Findings indicate the majority of districts in seismic zones III, IV, and V are low liquefiable, moderate liquefiable, and extremely liquefiable, respectively. Putti and Satyam [38] used the method described by IS 1893 (Part 1) as an effective tool for assessing the liquefaction susceptibility of Vishakhapatnam city in India.

According to the findings, the northern and central regions of the city are more vulnerable to liquefaction. These findings can help in retrofitting, analysis, and design of structures. Chanda et al. [39] examine the liquefaction potential using IS 1893 (Part 1): 2016 at Jaigarh Port in Ratnagiri, Maharashtra. The analysis reveals that fine sands with non-plastic silt with a high-water table pose the highest risk of liquefaction. Boulder formations with adequate drainage pathways resist liquefaction, while dense sands with moderate to high relative density exhibit good performance under strong shaking. Additionally, findings indicate that substrata beyond 15 meters depth pose lower liquefaction hazards, and rock formations serve as excellent subgrade for enduring periodic loads. Poddar et al. [40] employed a deterministic approach based on IS 1893 (Part 1): 2016 to estimate the likelihood of liquefaction potential in layered soil. By varying the PGA as a parameter, they demonstrated how different levels of ground shaking influence liquefaction susceptibility. This approach aids in understanding how seismic intensity interacts with soil behaviour to determine the liquefaction potential. Ghani et al. [41] delved into the liquefaction susceptibility of sites along the Ganga River bank. Employing the methodology outlined in IS 1893 (Part 1), they extended their analysis to incorporate a multi-linear regression model. Their investigation revealed that beyond FC, the plasticity of soil plays a crucial role in assessing liquefaction susceptibility.

Mittal et al. [42] compared SPT-based deterministic approaches. In Indian and US codes of practice, it is generally suggested that liquefaction evaluation may not be required if the SPT N-value is above a certain threshold. However, detailed analysis often reveals that the FS_L is lower than desired which indicates the need for re-evaluation. Satyam and Rao [43] initiated microzonation studies in the two major cities namely Delhi and Vijayawada in seismic zones IV and III respectively, as part of the initiative taken by the Department of Science and Technology, Government of India. They assessed the liquefaction potential using shear wave velocities and SPT borehole data. The assessments reveal severe liquefaction potential in certain areas of Delhi, particularly in the north and northeast, while Vijayawada faces a likelihood of liquefaction in locations like Patamata, Autonagar, and Kanuru. These findings are crucial for urban planning and safe construction practices to minimize future earthquake losses. Bhattacharya et al. [44] used the Seed's method [36] and the Andrus's method [45] for the assessment of the liquefaction

potential of the soil deposits in that area. A semi-empirical correlation between the SPT N value and the shear wave velocity in the Rajarhat area of Kolkata was established by them. They identified that the most sensitive parameters for calculating liquefaction potential were SPT blow count and PGA. They marked the end of the liquefiable zone approximately 15 meters below ground level as the subsoil was found to be non-liquefiable beyond this depth. Gurung and Chatterjee [46] evaluated the susceptibility of liquefaction of Kolkata employing deterministic approaches from Boulanger's [47] method and IS 1893 (Part 1): 2016 [4] method. The study found that with an increase in the depth of soil below ground level, liquefaction potential decreases but increases with earthquake magnitude (M_w). The IS 1893 (Part 1): 2016 method yielded higher FS_L values, indicating less risk of liquefaction. Kumar et al. [48] conducted an assessment of liquefaction potential sites within the AIIMS Kalyani, Kolkata Campus, utilizing SPT data. Their findings indicate a decrease in susceptibility to liquefaction with decreasing M_w at shallow depths. Furthermore, the study highlights the significant disparities between earthquakes of 7.0 and 7.5 magnitudes, with the latter exhibiting greater susceptibility.

In an effort to assess the vulnerability of cities against liquefaction, Naik and Patra [49] undertook a study focused on Kanpur and Allahabad. Utilizing a simplified procedure, they generated spatial distribution maps of liquefaction potential for these urban areas. The findings highlighted that both Kanpur and Allahabad are susceptible to liquefaction during earthquakes of moderate to large magnitudes. Muley et al. [50] assessed liquefaction potential in Roorkee, India using two methods: field-based on SPT N-Values [51] and lab-based on grain size distribution [36]. Results showed higher FS_L with the field approach compared to lab data. Ground response analysis [52] yielded significantly lower FS_L than simplified methods, indicating its insufficiency. Again Muley et al. [53] found the Tokimatsu and Youshimi method is useful for estimating the liquefaction potential within Roorkee, India. They computed the liquefaction potential for M_w 7.0 and PGA 0.24g. The study helps understand the establishment of liquefaction relations based on SPT and the potentially liquefiable sites. Dwivedi et al. [54] evaluated the liquefaction susceptibility of Ahmedabad using the deterministic [4, 36, 37] method based on the SPT-N value. They found that the city has densely compacted soil with low water table resulting in high SPT N-value and low

liquefaction. Although the analysis shows that the area is safe for building, thorough geotechnical studies are required for heavy engineering and high-rise projects. For the nuclear power plant foundation safety, Jha et al. [55] found that SPT-based empirical methods for liquefaction susceptibility are crucial. Based on the findings, they concluded that an FS_L of 1.0 does not ensure non-liquefaction incidents. Hore et al. [56] conducted an assessment of earthquake-induced liquefaction potential in specific reclaimed zones of Dhaka city, utilizing data from the Cone Penetration Test and SPT. Filling depths in these areas ranged from 1.5 to 13.5 meters below the existing ground level, considering a PGA of 0.15g and a M_w of 7.5 for the liquefaction analysis. Their findings indicate an increased risk of liquefaction zones filled with dredged soil, particularly within depths of 1.5 to 4.5 meters. The evaluation of liquefaction potential, based on both CPT and SPT data, demonstrates varying levels of susceptibility across different locations. Typically, areas with lower liquefaction potential are found along the central and north-south axes of Dhaka City, while zones with higher potential are situated towards the outer periphery. In their study, Patriaman et al. [57] assessed the liquefaction susceptibility of the Palu-Bay coastal region in the Central Sulawesi Province using the simplified procedure method. Geological observations revealed a predominance of non-cohesive soil (sand) in the Palu Bay area. Results indicated that while the eastern region showed minimal liquefaction potential, the western and southern parts exhibited significantly higher liquefaction potentials. Wadi et al. [58] assessed the subsurface formation for soil liquefaction analysis at a sugar plant located in the Upper Benue region of Nigeria using the SPT data. Assuming $M_w=7.5$ and a PGA of 0.15 g, assessments were conducted by the deterministic technique [47]. The findings show that sandy, silty, clayey, saturated loose to medium-dense soil with $FS_L < 1$ is found in the range of 1.5–4.5 m depth. The very thick to stiff clayey sands in deeper strata (beyond 4.5 meters) have an $FS_L > 1$. They found the method is effective for evaluating the liquefaction of sandy soil under the influence of earthquakes. Using the deterministic approaches, Nilay et al. [59] conducted a study to assess liquefaction susceptibility at the IIT Patna campus using in-situ soil properties like SPT-N, cone penetration resistance value, and shear wave velocity. They generated hazard maps considering all three types of field test results. Their findings indicate that the IIT Patna Campus can benefit from the cone penetration resistance-based method in conjunction

with a thorough strategy for analyzing liquefaction potential in soils with high fines concentration. Ansari et al. [60] examine the soil liquefaction susceptibility of the Jammu area in the northwest Himalayas. They identify areas near the Tawi and Ravi rivers as highly susceptible to liquefaction due to young alluvium deposits, while other regions are less prone due to factors like high shear wave velocities or thick sand deposits. Ortiz-hernández et al. [61] performed an investigation to evaluate the liquefaction potential in Portoviejo, Ecuador, in the aftermath of the 2016 Pedernales earthquake, utilizing field data based on SPT. Their analysis identified areas with a heightened likelihood of liquefaction, particularly within the urban core. They pinpointed strata at depths ranging from 8 to 12 meters as potentially susceptible to liquefaction. Conversely, regions in the southeast of the city, characterized by older sedimentary deposits, exhibited a reduced susceptibility to liquefaction. These findings are consistent with the observed environmental impacts following the earthquake.

Deviprasad et al. [62] compared deterministic liquefaction assessment methods with probabilistic methods for saturated silty sand. The deterministic methods include Indian Standards [4] and European Standards [63], as well as the Boulanger and Idriss method [47] whereas, probabilistic evaluation [64] involves Monte Carlo simulation and literature-based preliminary liquefaction probability estimation. The Boulanger and Idriss method demonstrated higher accuracy due to updated case histories and datasets. While other deterministic approaches yield similar FS_L , probabilistic analysis uncovers varying failure probabilities. Acharya et al. [65] assess the liquefaction susceptibility of Kathmandu Valley, Nepal, using the deterministic approach. They found that most areas in the valley are moderately to highly susceptible to liquefaction, particularly the southern and central regions posing higher risks than the northern sections. These findings underscore the importance of the evaluation of liquefaction potential to ensure the safety of engineered structures in this heavily populated metropolitan area.

Aytaş et al. [66] examined the soil liquefaction susceptibility in Turkey's Batman Settlement Zone, situated close to the East Anatolian Fault Zone. The study utilized methodologies based on SPT and shear wave velocity. They analyzed soil at two sites, Meydan and Bahçelievler, considering M_w 7.5 and 6.5 and PGA of 0.30 g. According to their findings, it is essential to take into consideration both soil and

seismic factors for more accurate assessments of liquefaction potential. Additionally, the areas with high liquefaction risk were associated with significant total settlements which indicate potential high settlements in those regions. Kundu et al. [67] conducted a study on the liquefaction potential and risk assessment of the Gautam Buddha Nagar district in Uttar Pradesh, India. Employing the SPT-based deterministic approach, they identified a high vulnerability zone in the central region of the selected area.

Tokimatsu and Youshimi [35] proposed a relationship between the corrected dynamic shear stress ratio and normalized SPT N -values with a focus on the fines content and SPT N -values. According to the recognized relationship, they found that sands with above 10 percent fines exhibit more resistance to liquefaction than clean sands with equal SPT N -values. Less likely to sustain substantial damage are clean sands with SPT N_1 -values above 25, silty sands with more than 10% fines and SPT N_1 -values above 20, or sandy silts with more than 20% clay. Furthermore, as compared to clean sands with similar SPT N_1 -values, sands with gravel particles show less resistance to liquefaction. They also provided an enhanced empirical chart that uses the dynamic shear stress ratio, SPT N_1 -values, fines content, and shear strain amplitude to distinguish between liquefiable and non-liquefiable circumstances. A thorough review of SPT- N -based techniques was carried out by Hwang and Yang [68] utilizing 302 liquefiable as well as non-liquefiable cases from the Chi-Chi Earthquake of 1999. For this assessment, the safety factor error and the success rate are used as indices. The results show that Seed's approach is the most accurate and has the highest success rate, while Tokimatsu's method is the next most accurate. Chang et al. [69] investigated the stability and precision of SPT- N -based techniques for liquefaction evaluation in the aftermath of Taiwan's Chi-Chi earthquake. The most sensitive factors in liquefaction potential computation are found to be SPT blow count and PGA. The study finds that the Tokimatsu's method is more accurate. Subası and İkizler [70] conducted a study to determine the liquefaction susceptibility in the Erzincan city centre and its surroundings, considering earthquake scenarios produced using three empirical methods viz. Seed's [36] method, Tokimatsu's [35] method, and Iwasaki et al. [71] method. In his study, the area containing clayey soil has been excluded. Results show an agreement that the liquefaction potential characteristics are increased by sandy-silty soils,

groundwater, and its combination. In his study, the area containing clayey soil has been excluded.

Turning into a neighbouring country, Rahman et al. [72] employed the Tokimatsu and Youshimi method to assess the liquefaction severity of Chattogram, the second-largest city in Bangladesh. They created a hazard map to identify high and low liquefaction risk areas which can be used as a guide for disaster management authority. Hossain et al. [73] also conducted a study in the northwestern region of Bangladesh. They used the deterministic approach proposed by Tokimatsu and Youshimi to evaluate the liquefaction potential. The positive outcomes of their study underscore the applicability of this approach in different geographic and geological regions. This study contributes to the understanding of potential liquefaction impacts in densely populated urban environments.

Geographical information system (GIS) technology has also played a pivotal role in assessing liquefaction susceptibility. A GIS-based liquefaction susceptibility map was created by Mhaske et al. [74] for Mumbai City. According to their studies, existing soil strata often include over 50% clay and have high liquid and plastic indices, rendering them prone to liquefaction. Anbazhagan et al. [75] assessed and mapped the liquefaction potential of Chennai, India, using the SPT-based deterministic approach. According to their study, the eastern part of their study area was found to be more liquefiable. Ganapathy et al. [76] also utilized GIS-based methods to map the liquefaction susceptibility of soils in Chennai, aiding in urban planning and disaster preparedness. The study reveals that 60 % of the areas having alluvial deposits are at risk of liquefaction during moderate earthquakes, as saturated sediment compacts during shaking. Das et al. [77] harnessed GIS to create a liquefaction potential map for Agartala, a state in northeastern India. Using the SPT borehole data, they conducted an analysis and discovered that the potential in the central, southern, and northern parts of the state is high to moderate, low to non-liquefiable, and moderate to non-liquefiable, respectively. The Sabarmati River basin in Gujarat State, India, was studied by Bhatt et al. [78]. To produce a seismic hazard map, they gathered data on geology, tectonics, seismicity, and shear-wave velocity and combined it with a GIS platform. Based on the map, the seismic danger is highest in the southeastern, moderate in the central, and lowest in the northeastern part of the Aravalli Range. The results imply that urban planners

can benefit from having a macro-level seismic hazard map.

A study conducted by Satyanarayana et al. [79] focused on the liquefaction susceptibility of subsoil strata along the Visakhapatnam coastal area. Utilizing IS 1893 (Part 1), the researchers divided the area into different seismic zones. The results indicated that while areas within zone II were less susceptible to liquefaction, those falling within zones IV and V exhibited a higher vulnerability. Boumpoulis et al. [80] assessed the soil liquefaction potential in the coastal area of the Gulf of Patras, Greece, focusing on regions affected by liquefaction following a 2008 earthquake using the SPT and cone penetration test data. These values were integrated into GIS to generate liquefaction hazard maps using interpolation methods. The evaluation was performed for three earthquake scenarios, revealing varying levels of liquefaction susceptibility. The study suggests that an earthquake of $M_w = 6.5$ and $PGA = 0.24g$ poses the most significant risk of damage to existing structures and infrastructure. Similarly, Rawat et al. [81] utilized GIS tools to map liquefaction susceptibility across the east Ganga plain, offering spatial insights into the regions prone to liquefaction hazards. The study found that Gandak and Mahananda are immensely active, while Bagmati, Burhi Gandak, and Kosi are middlingly active.

The application of GIS extended to other urban contexts as well. A GIS-based multi-criteria method was adopted by Pancholi et al. [82] to examine the macro-level seismic hazard in Kachchh, Gujarat. The study reveals that the huge land areas are vulnerable to liquefaction hazards, and seismic microzonation is necessary for the Bhuj, Bhachau, and Rapar corridors. According to a study, there is low risk in the southwest and moderate to high risk in the middle and northern regions of the Kachchh mainland. Ashikuzzaman et al. [83] assessed the vulnerability of Rajshahi City Corporation to earthquake liquefaction using the simplified method. Based on the result, they mapped using ArcGIS for visualization and categorized the area into four liquefaction severity levels. This study provides valuable insights for engineers and planners to develop structural schemes in the region. These studies highlight the role of GIS in facilitating comprehensive hazard assessment.

2.1 Summary of literature review

Based on the literature review presented, the following point is worth noting:

- The study emphasizes the need for urban planning and construction practices.
- Currently, there is a lack of comprehensive studies for seismic soil liquefaction in Bihar.
- IS 1893 (Part 1): 2016, and Tokimatsu and Yoshimi (1983) have been proven to be effective tools for liquefaction susceptibility assessment.
- GIS has been proven to be a useful mapping software to describe the severity of liquefaction.
- FC, SPT blow count, depth of water table, and PGA are the main influencing factors for soil liquefaction phenomena.

Collectively, these studies underscore the methodologies and tools employed to assess liquefaction potential and susceptibility across different regions for effective urban planning and disaster mitigation strategies. Despite the importance of understanding soil liquefaction and earlier research in this field, there is currently a lack of comprehensive studies that provide detailed information on the soil liquefaction potential in Bihar. Most existing studies have focused on other areas or used limited data sources, which may not accurately represent the actual subsurface conditions in Bihar. Therefore, there is a need for a thorough investigation of the liquefaction susceptibility of soil in Bihar based on actual subsurface data. The present study aimed to fill this gap by investigating the liquefaction susceptibility of all 38 districts in Bihar. ArcGIS 10.8 (2019) software was utilized to create a liquefaction hazard zonation map of the study area at different depths below the ground surface. A liquefaction hazard zonation map can serve as a guide for local as well as government bodies in planning and designing buildings and infrastructure in Bihar. This paper provides valuable insights into the actual subsurface conditions, which can aid future researchers in further investigating soil liquefaction in this region.

3.Methods

The liquefaction susceptibility of soil is measured by the FS_L value. The deterministic method, known as the "Simplified Procedure," was introduced by Seed and Idriss (1971) [36]. Over time, researchers have proposed numerous corrections and strategies to enhance the accuracy of predictions. In this study, two deterministic methods, namely Tokimatsu and Yoshimi, 1983 [35], and IS 1893 (Part 1): 2016 [4], have been employed, which are based on SPT test data. The following section describes the various steps involved. Equations 2 to 14 are presented for IS 1893 (Part 1): 2016 method, whereas Equations (15)

to (21) are presented for Tokimatsu and Yoshimi, 1983 method.

(a)IS 1893 (Part 1): 2016 method

$$CSR = 0.65 \left(\frac{a_{max}}{g} \right) \left(\frac{\sigma_{vo}}{\sigma'_{vo}} \right) r_d \quad (2)$$

$$r_d = \begin{cases} 1 - 0.00765z & 0 < z \leq 9.15m \\ 1 \cdot 174 - 0.0267z & 9.15m < z \leq 23.0m \end{cases} \quad (3)$$

Where, factor 0.65 in Equation (2) is used as a reference stress level by Seed and Idriss [84], which was kept the same in IS 1893 (Part 1): 2016 method; a_{max} = PGA (0.16g, 0.24g, and 0.36g for zones III, IV, and V respectively); g = Acceleration due to gravity; r_d is the stress reduction factor for depth (z).

$$CRR = CRR_{7.5}(MSF)K_{\sigma}K_{\alpha} \quad (4)$$

$$\text{Where, } CRR_{7.5} = \frac{1}{34 - (N_1)_{60cs}} + \frac{(N_1)_{60cs}}{135} + \frac{50}{[10 \times (N_1)_{60cs} + 45]^2} - \frac{1}{200} \quad (5)$$

$$(N_1)_{60cs} = \alpha + \beta(N_1)_{60} \quad (6)$$

$$\alpha = \begin{cases} \alpha = 0 \beta = 1 \text{ for } FC \leq 5\% \\ e^{[1.76 - \frac{190}{FC^2}]} \beta = 0.99 + \frac{FC^{1.5}}{1000} \text{ for } 5\% < FC < 35\% \\ \alpha = 0.5 \beta = 1.2 \text{ for } FC \geq 35\% \end{cases} \quad (4)$$

$$(N_1)_{60} = C_N N_{60} \quad (5)$$

$$C_N = (P_a / \sigma'_{vo})^{0.5} \leq 1.7 \quad (6)$$

$$N_{60} = N C_{60} \quad (7)$$

$$C_{60} = C_{HT} C_{HW} C_{SS} C_{RL} C_{BD} \quad (8)$$

$$MSF = 10^{2.24 / M_w^{2.56}} \quad (9)$$

$$N_{60} = N C_{60} \quad (10)$$

$$C_{60} = C_{HT} C_{HW} C_{SS} C_{RL} C_{BD} \quad (11)$$

$$MSF = 10^{2.24 / M_w^{2.56}} \quad (12)$$

$$K_{\sigma} = (\sigma'_{vo} / P_a)^{f-1} \quad (13)$$

$$f = \begin{cases} 0.8 \sim 0.7 \text{ For } D_r = 40\% \text{ to } 60\% \\ 0.7 \sim 0.6 \text{ For } D_r = 60\% \text{ to } 80\% \end{cases} \quad (14)$$

Where, N_{60} , $(N_1)_{60}$, and $(N_1)_{60cs}$ are SPT N-value normalized for hammer efficiency, for overburden stress and FC respectively; C_N and C_{60} are correction factor overburden stress and hammer efficiency respectively; MSF is the magnitude scaling factor; M_w is the magnitude of an earthquake on Richter scale; K_{σ} is the correction for high overburden stresses (depth >15m) and K_{α} are correction for static shear stress (only for sloping ground); P_a is atmospheric pressure in kPa and f is an exponent (depends on the relative density of soil, D_r); C_{HT} , C_{HW} , C_{SS} , C_{RL} , and C_{BD} are the correction factors for non-standard SPT accounted for hammer type,

hammer weight, sampler type, rod length, and borehole diameter respectively. The values of these factors have been taken following IS 1893 (Part 1): 2016, as given in Table 4 and 5.

(b) Tokimatsu and Yoshimi, 1983 method

$$CSR = \left(\frac{a_{max}}{g}\right) \left(\frac{\sigma_{vo}}{\sigma'_{vo}}\right) r_d r_n \tag{15}$$

$$r_n = 0.1(M_w - 1) \tag{16}$$

$$r_d = 1 - 0.015z \tag{17}$$

Where, r_n is earthquake magnitude correction factor.

$$CRR = a C_r \left[\frac{16\sqrt{N_a}}{100} + \left(\frac{16\sqrt{N_a}}{C_s}\right)^n \right] \tag{18}$$

$$C_s = \begin{cases} 75 & \text{for extensive liquefaction} \\ 80 & \text{for liquefaction} \\ 90 & \text{for no liquefaction} \end{cases} \tag{19}$$

Where, $C_r = 0.57$ is the correction factor proposed by Alba et al. [85] on account of the lack of high quality of the undisturbed soil sample. Empirical parameter C_s is added on account of the strain amplitude of reconstituted sand. Empirical constants $a = 0.45$ and $n = 14$ are used in Equation (18) to give a reasonably linear plot on a semi-log graph between strain amplitude and C_s [35]. In the current investigation, the value of the empirical parameter C_s has been set to 80 from Equation (19).

$$N_a = N_1 + \Delta N_f \tag{20}$$

$$N_1 = C_N N = \frac{1.7}{\sigma'_{vo} \left(\frac{kgf^2}{cm}\right)^{+0.7}} N \tag{21}$$

Where, N_a is the adjusted SPT N-value; N_1 is the normalized SPT N-value for overburden stress, C_N is the overburden correction factor and ΔN_f is the correction factor for FC. It can be interpolated from the Table 3 below.

Table 3 Fines content correction

FC (%)	ΔN_f
0-5	0
5-10	Interpolate
10-	0.1FC+4

The present study is based on the utilization of SPT test data. Therefore, the two deterministic methodologies given by Tokimatsu and Yoshimi (1983), and IS 1893 (Part 1): 2016 have been used in the current study. An interesting point is noted here that in the case of Tokimatsu and Yoshimi's (1983) method, a linear earthquake magnitude correction factor, i.e. r_n , is applied in the expression of CSR, whereas in the IS 1893 (Part 1): 2016 method, an earthquake magnitude scaling factor, i.e., MSF, is applied while computing the CRR to obtain the liquefaction resistance. In the IS 1893 (Part 1): 2016 method, the magnitude weighting factor, which is the inverse of MSF, may be applied to correct CSR rather than MSF to correct CRR. The flow charts of the above two methods are shown in Figures 2 and 3.

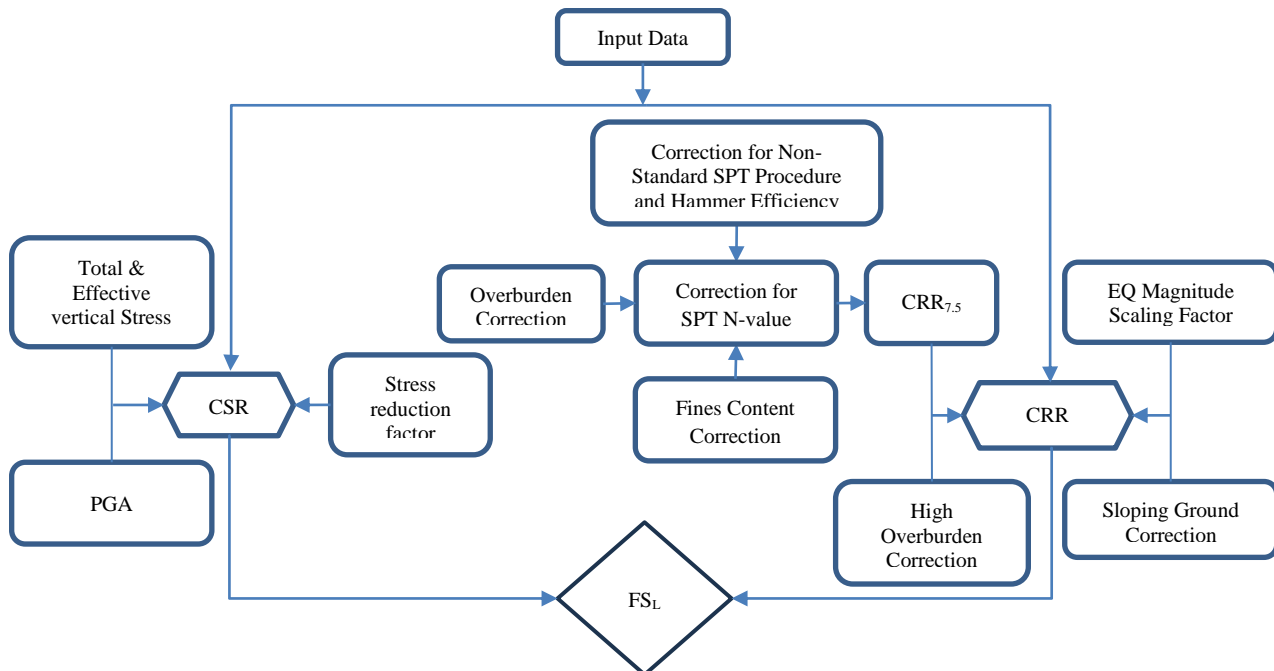


Figure 2 Flow chart of IS 1893 (Part 1): 2016 method

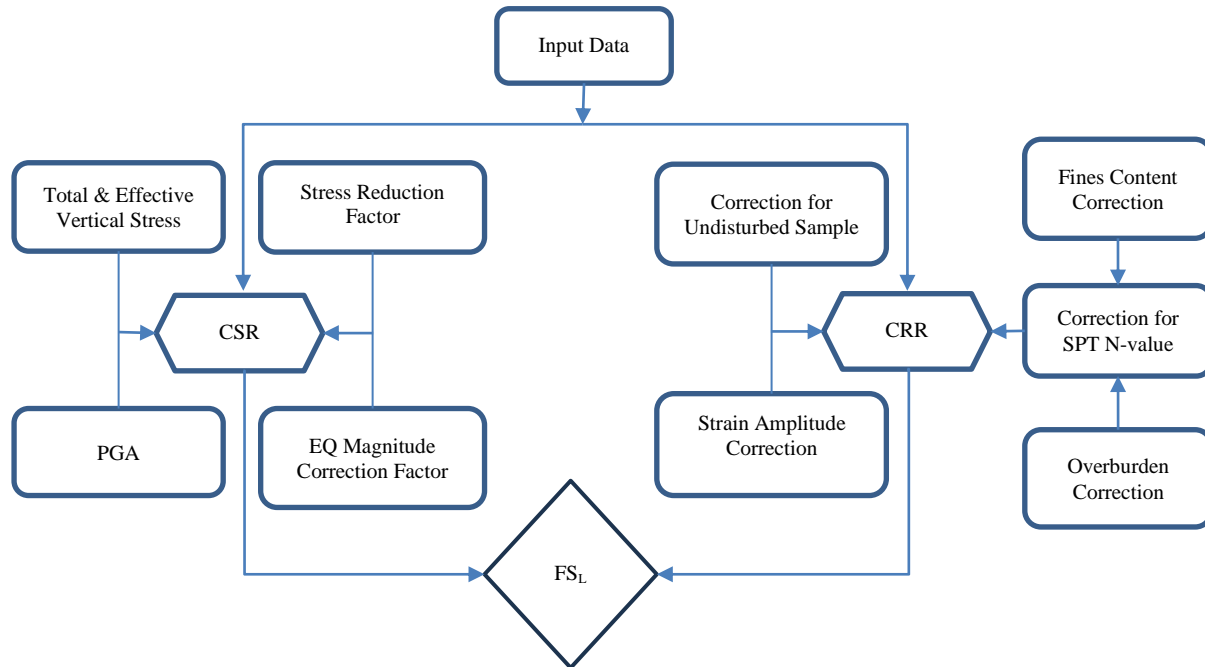


Figure 3 Flow chart of Tokimatsu and Yoshimi, 1983 method

4.Results

Based on the method described in Section 3, analysis was performed in a spreadsheet, and the graph was plotted to study the variations. To investigate the effect of the varying magnitude of an earthquake on the soil liquefaction potential, $M_w = 6.0, 6.5, 7.0,$ and 7.5 have been taken in this project. Equation 1 shows that FS_L is inversely proportional to CSR. So, attempts have been made to make the worst combination of soil liquefaction susceptibility in Bihar. Due to the fluctuating water table throughout the year, it has been assumed to be on the ground surface to get the lowest value of effective stress, σ'_{vo} . A typical calculation for IS 1893 (Part 1): 2016 method has been presented in *Tables 4 to 5*, and the Tokimatsu and Yoshimi (1983) method has been presented in *Tables 6 to 7* in correlation with the typical soil profile of the East Champaran district given in *Table 1*. The FS_L values of the two methods employed in this study with different magnitudes of earthquakes are shown in *Table 8*. The variation of SPT values with depth is depicted in *Figure 4*, and the variation of FS_L with depth and M_w is depicted in *Figures 5 and 6*. *Figures 7 and 8* show the variation of CRR with FC, whereas *Figures 9 and 10* show the variation of CRR with a normalized SPT blow count. *Figure 11* gives the comparison between the FS_L values from the two methods.

Tables 4 and 5 show the typical calculation of FS_L according to the methodology given in IS 1893 (Part 1): 2016, whereas *Tables 6 and 7* show the typical calculation according to the Tokimatsu and Yoshimi (1983) method. *Figures 4, 5, 6,* and *Table 8* illustrate a comparison between the FS_L values of two specified methodologies. It may be noted here that the FS_L value decreases with increasing M_w in both methods. There is a sudden increase in FS_L value that can be seen at 10.5 m to 12.0 m and at 16.5 m depth. This is due to the increase in the SPT value. At higher depths below 15 m, the FS_L value is greater than 1. It means that the soil is more resistant to liquefaction at higher depths.

Figures 7 and 8 show the variation of liquefiable and non-liquefiable soil with the normalized SPT N-value and FC for IS 1893 (Part 1): 2016 and the Tokimatsu and Yoshimi (1983) methods, respectively. The result indicates that the specific combination of FC and SPT N-value determines the liquefaction susceptibility of soil. IS 1893 (Part 1): 2016 method indicates soil liquefies most for FC above 20% when $(N_1)_{60}$ is within 20, while for FC between 10% and 20%, liquefaction occurs over a wider range of $(N_1)_{60}$ values up to 25, and FC below 10% has a higher liquefaction susceptibility, reaching $(N_1)_{60}$ values up to 30.

However, Tokimatsu and Yoshimi's (1983) method indicates higher chances of liquefaction for FC above 10% when N_1 values up to 15 and FC below 10% when N_1 values up to 25. The outcome demonstrates

that as FC increases at a constant SPT N-value, the FS_L value increases as well.

4.1 Typical calculations and graphs

Table 4 Typical Correction factor of SPT N- value for a borehole (L13) in East Champaran district as per IS 1893 (Part 1): 2016

Depth (m)	SPT N-value	C_N	C_{HT}	C_{HW}	C_{SS}	C_{RL}	C_{BD}	C_{60}	N_{60}	$(N_1)_{60}$	$(N_1)_{60CS}$
1.5	8	1.70	0.75	1.00	1.10	0.75	1.05	0.65	5.20	8.84	12.38
3.0	11	1.70	0.75	1.00	1.10	0.80	1.05	0.69	7.62	12.96	16.08
4.5	7	1.70	0.75	1.00	1.10	0.85	1.05	0.74	5.15	8.76	11.34
6.0	13	1.46	0.75	1.00	1.10	0.95	1.05	0.82	10.70	15.59	19.86
7.5	13	1.30	0.75	1.00	1.10	0.95	1.05	0.82	10.70	13.94	18.10
9.0	16	1.19	0.75	1.00	1.10	0.95	1.05	0.82	13.17	15.67	18.92
10.5	23	1.10	0.75	1.00	1.10	1.00	1.05	0.87	19.92	21.95	25.50
12.0	24	1.00	0.75	1.00	1.10	1.00	1.05	0.87	20.79	20.78	25.40
13.5	12	0.94	0.75	1.00	1.10	1.00	1.05	0.87	10.40	9.80	13.68
15.0	17	0.89	0.75	1.00	1.10	1.00	1.05	0.87	14.73	13.17	17.83
16.5	30	0.85	0.75	1.00	1.10	1.00	1.05	0.87	25.99	22.16	27.53
18.0	26	0.82	0.75	1.00	1.10	1.00	1.05	0.87	22.52	18.38	23.75
20.5	28	0.76	0.75	1.00	1.10	1.00	1.05	0.87	24.26	18.55	23.93
25.0	28	0.69	0.75	1.00	1.10	1.00	1.05	0.87	24.26	16.80	21.75
30.0	30	0.63	0.75	1.00	1.10	1.00	1.05	0.87	25.99	16.43	20.75

Table 5 Typical calculation of FS_L of a borehole (L13) in East Champaran district as per IS 1893 (Part 1): 2016 for $M_w=7.5$

Depth(m)	r_d	M_w	MSF	$\frac{a_{max}}{g}$	CSR	f	P_a (kPa)	K_σ	K_α	CRR _{7.5}	CRR	FS_L
1.5	0.99	7.5	1	0.24	0.36	0.7	100	1.00	1	0.13	0.13	0.377
3.0	0.98	7.5	1	0.24	0.35	0.7	100	1.00	1	0.17	0.17	0.485
4.5	0.97	7.5	1	0.24	0.35	0.7	100	1.00	1	0.13	0.13	0.359
6.0	0.95	7.5	1	0.24	0.33	0.7	100	1.00	1	0.21	0.21	0.638
7.5	0.94	7.5	1	0.24	0.33	0.7	100	1.00	1	0.19	0.19	0.583
9.0	0.93	7.5	1	0.24	0.33	0.7	100	1.00	1	0.20	0.20	0.619
10.5	0.89	7.5	1	0.24	0.31	0.7	100	1.00	1	0.30	0.30	0.963
12.0	0.85	7.5	1	0.24	0.29	0.7	100	1.00	1	0.30	0.30	1.034
13.5	0.81	7.5	1	0.24	0.28	0.7	100	1.00	1	0.15	0.15	0.532
15.0	0.77	7.5	1	0.24	0.26	0.7	100	0.94	1	0.19	0.18	0.676
16.5	0.73	7.5	1	0.24	0.25	0.7	100	0.91	1	0.35	0.32	1.291
18.0	0.69	7.5	1	0.24	0.24	0.7	100	0.89	1	0.27	0.24	1.011
20.5	0.63	7.5	1	0.24	0.21	0.7	100	0.85	1	0.27	0.23	1.089
25.0	0.51	7.5	1	0.24	0.17	0.7	100	0.80	1	0.24	0.19	1.112
30.0	0.37	7.5	1	0.24	0.13	0.7	100	0.76	1	0.23	0.17	1.349

Table 6 Typical Correction factor of SPT N- value for a borehole (L13) in East Champaran district as per Tokimatsu and Yoshimi, 1983

Depth (m)	SPT N-value	C_N	N_1	ΔN_f	N_a
1.5	8	2.09	16.71	5.70	22.41
3.0	11	1.83	20.15	5.50	25.65
4.5	7	1.63	11.42	5.40	16.82
6.0	13	1.44	18.72	5.80	24.52
7.5	13	1.31	16.99	5.80	22.79
9.0	16	1.20	19.15	5.50	24.65
10.5	23	1.10	25.38	5.50	30.88
12.0	24	0.99	23.71	5.80	29.51

Depth (m)	SPT N-value	C _N	N ₁	ΔN _f	N _a
13.5	12	0.92	11.03	5.80	16.83
15.0	17	0.86	14.62	6.00	20.62
16.5	30	0.81	24.24	6.00	30.24
18.0	26	0.76	19.81	6.10	25.91
20.5	28	0.70	19.47	6.10	25.57
25.0	28	0.60	16.84	6.00	22.84
30.0	30	0.52	15.68	5.80	21.48

Table 7 Typical calculation of FS_L of a borehole (L13) in East Champaran district as per Tokimatsu and Yoshimi, 1983 for M_w=7.5

Depth (m)	r _d	M _w	r _n	$\frac{a_{max}}{g}$	CSR	a	n	C _r	C _s	CRR	FS _L
1.5	0.98	7.5	0.65	0.24	0.35	0.45	14	0.57	80	0.31	0.887
3.0	0.96	7.5	0.65	0.24	0.35	0.45	14	0.57	80	0.51	1.491
4.5	0.93	7.5	0.65	0.24	0.34	0.45	14	0.57	80	0.18	0.547
6.0	0.91	7.5	0.65	0.24	0.32	0.45	14	0.57	80	0.43	1.338
7.5	0.89	7.5	0.65	0.24	0.31	0.45	14	0.57	80	0.33	1.060
9.0	0.87	7.5	0.65	0.24	0.30	0.45	14	0.57	80	0.44	1.435
10.5	0.84	7.5	0.65	0.24	0.30	0.45	14	0.57	80	1.35	4.572
12.0	0.82	7.5	0.65	0.24	0.28	0.45	14	0.57	80	1.04	3.740
13.5	0.80	7.5	0.65	0.24	0.27	0.45	14	0.57	80	0.18	0.681
15.0	0.78	7.5	0.65	0.24	0.26	0.45	14	0.57	80	0.25	0.962
16.5	0.75	7.5	0.65	0.24	0.26	0.45	14	0.57	80	1.20	4.687
18.0	0.73	7.5	0.65	0.24	0.25	0.45	14	0.57	80	0.54	2.171
20.5	0.69	7.5	0.65	0.24	0.24	0.45	14	0.57	80	0.51	2.162
25.0	0.63	7.5	0.65	0.24	0.21	0.45	14	0.57	80	0.33	1.566
30.0	0.55	7.5	0.65	0.24	0.19	0.45	14	0.57	80	0.28	1.493

Table 8 FS_L of a borehole (L13) in East Champaran district, Bihar for M_w=6.0, M_w=6.5, M_w=7.0, and M_w=7.5

Depth (m)	IS 1893 (Part 1): 2016				Tokimatsu and Yoshimi, 1983			
	M _w =6.0	M _w =6.5	M _w =7.0	M _w =7.5	M _w =6.0	M _w =6.5	M _w =7.0	M _w =7.5
1.5	0.668	0.544	0.450	0.377	1.154	1.049	0.961	0.887
3.0	0.858	0.699	0.578	0.485	1.939	1.762	1.615	1.491
4.5	0.635	0.517	0.428	0.359	0.711	0.646	0.593	0.547
6.0	1.129	0.920	0.761	0.638	1.739	1.581	1.449	1.338
7.5	1.032	0.841	0.696	0.583	1.378	1.253	1.148	1.060
9.0	1.096	0.893	0.738	0.619	1.866	1.696	1.555	1.435
10.5	1.705	1.389	1.149	0.963	5.944	5.404	4.953	4.572
12.0	1.831	1.492	1.234	1.034	4.862	4.420	4.052	3.740
13.5	0.942	0.768	0.635	0.532	0.886	0.805	0.738	0.681
15.0	1.197	0.975	0.806	0.676	1.250	1.137	1.042	0.962
16.5	2.286	1.862	1.541	1.291	6.093	5.539	5.078	4.687
18.0	1.791	1.459	1.207	1.011	2.822	2.565	2.352	2.171
20.5	1.928	1.570	1.299	1.089	2.810	2.555	2.342	2.162
25.0	1.969	1.604	1.327	1.112	2.035	1.850	1.696	1.566
30.0	2.388	1.946	1.610	1.349	1.941	1.765	1.618	1.493

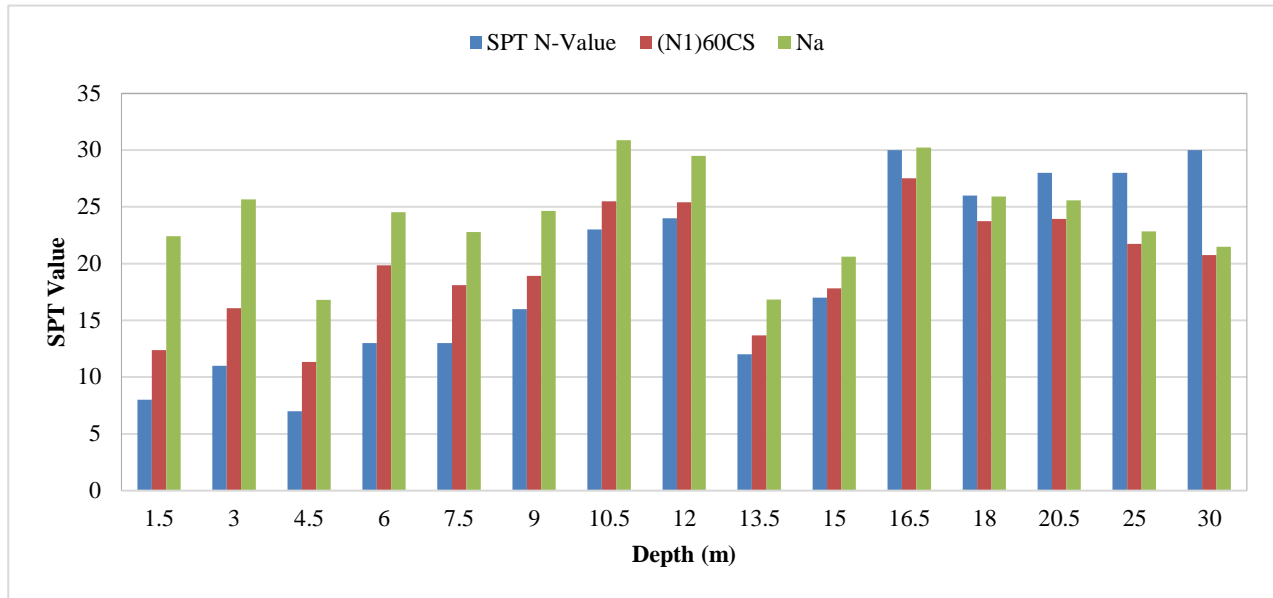


Figure 4 Plot of depth versus SPT value- N, $(N_1)_{60cs}$ and N_a

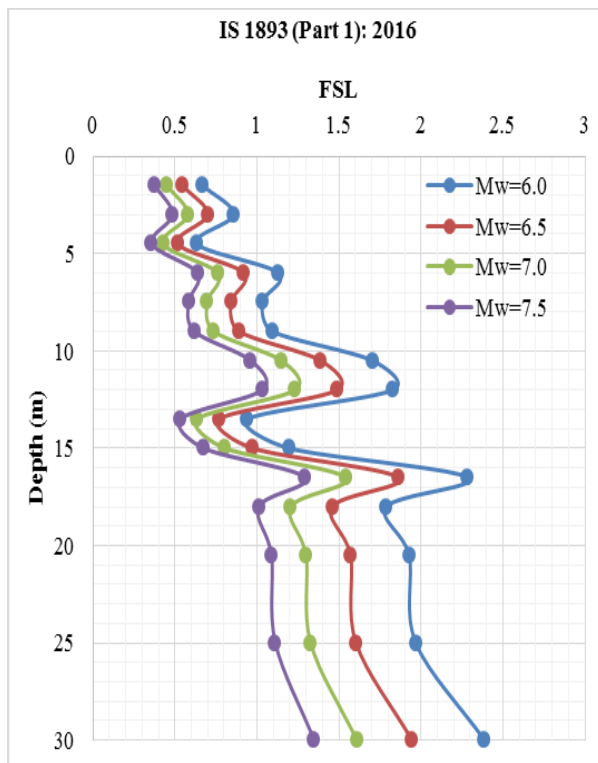


Figure 5 Typical plot of depth versus FS_L for a borehole (L13) in East Champaran district as per IS 1893 (Part 1): 2016

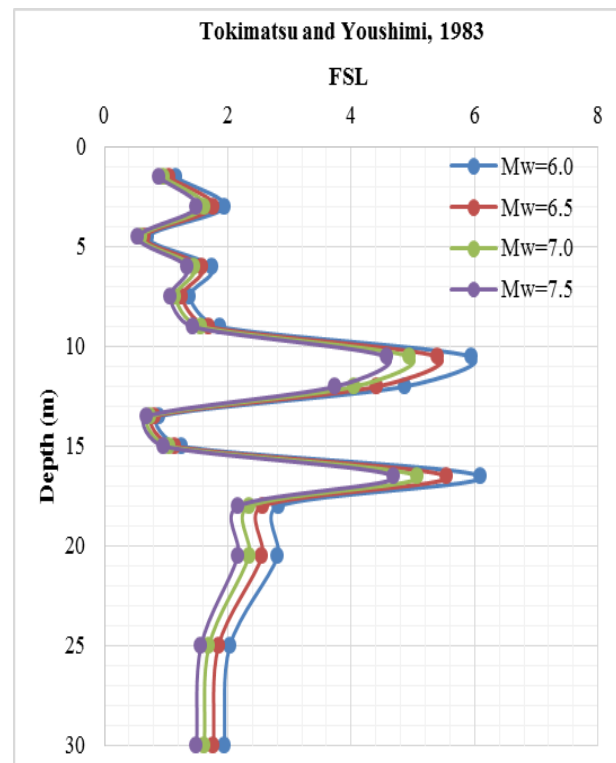


Figure 6 Typical plot of depth versus FS_L for a borehole (L13) in East Champaran district as per Tokimatsu and Yoshimi, 1983

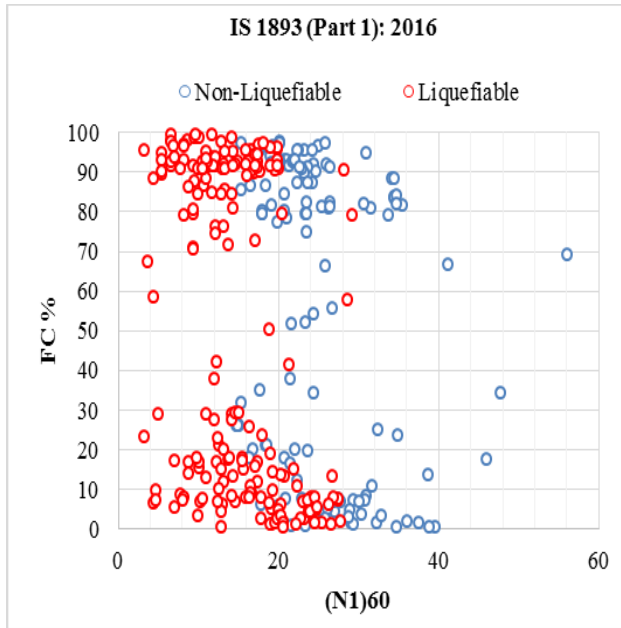


Figure 7 Plot of FC and normalized SPT blow count as per IS 1893 (Part 1): 2016 for $M_w=7.5$.

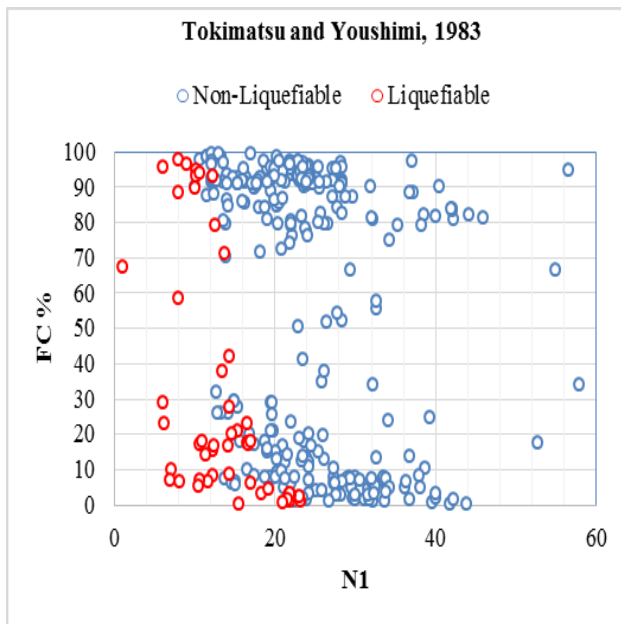


Figure 8 Plot of FC and normalized SPT blow count as per Tokimatsu and Youshimi, 1983 for $M_w=7.5$.

Figures 9 and 10 show the variation of liquefiable and non-liquefiable soils with normalized SPT N -values for overburden stress on the abscissa and CRR on the ordinate. A definite pattern of actual data can be visualized, showing different intercepts with the two methods. The IS 1893 method shows a clear intercept of about 0.05 on the ordinate, whereas the

Tokimatsu and Yoshimi methods are asymptotic towards the origin, giving an intercept of about 0.1 on the ordinate.

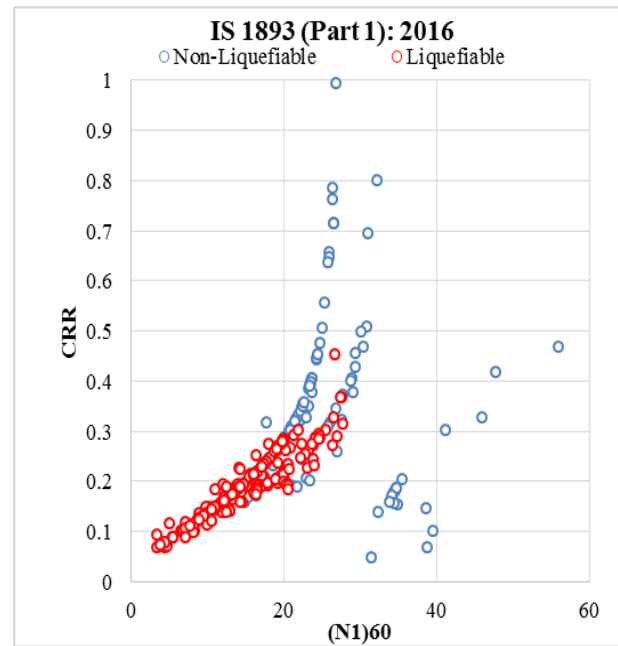


Figure 9 Relation between CRR and normalized SPT blow count as per IS 1893 (Part 1): 2016 for $M_w 7.5$.

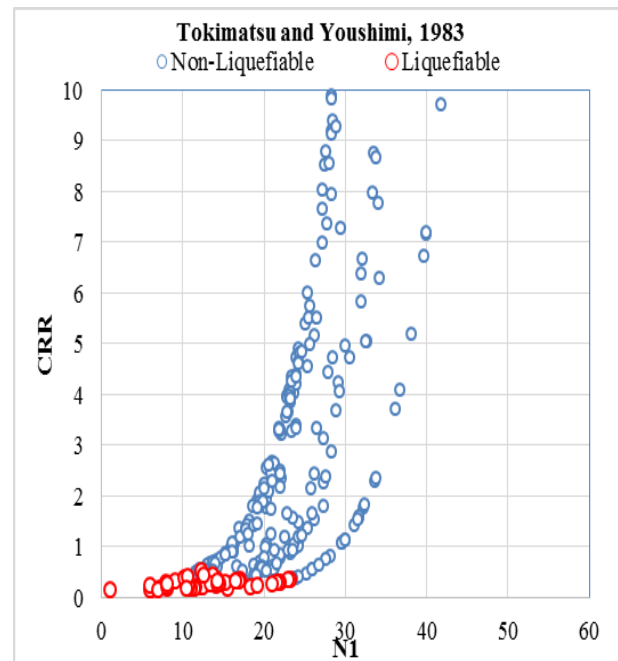


Figure 10 Relation between CRR and normalized SPT blow count as per Tokimatsu and Yoshimi, 1983 for $M_w=7.5$

The comparison of FS_L values for the two methodologies used in this study is shown in *Figure 11*. It shows a variation of the FS_L with the depth of soil below ground level. Here, it is observed that most of the FS_L values are within 4 as in the case of IS 1893 (Part 1): 2016 method, whereas they vary up to larger values in the case of Tokimatsu and Yoshimi (1983). It means that the FS_L converges more with the IS 1893 (Part 1): 2016 method.

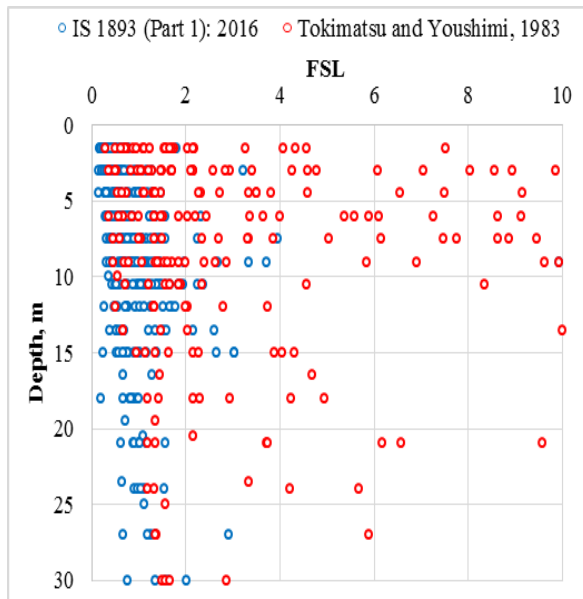


Figure 11 Plot of the depth versus FS_L for $M_w=7.5$

4.2 Hazard zonation map

Based on the above findings, hazard zonation maps have been provided in this section. Hazard zonation maps provide valuable insights into the liquefaction susceptibility of Bihar at different depths and M_w . The findings emphasize the importance of considering the depth and earthquake magnitude when assessing liquefaction hazards. It also underlines the significance of implementing appropriate engineering measures and construction practices to enhance the stability of the soil and minimise the risks associated with liquefaction in the region. It has been shown in *Figures 12 to 21*.

The hazard zonation maps presented in *Figures 12 to 21* depict the distribution of liquefaction susceptibility in Bihar at various depths (1.5 m, 3.0 m, 6.0 m, 9.0 m, and 15.0 m) below ground level. The maps were prepared using ArcGIS 10.8 (2019) and considered four M_w values: 6.0, 6.5, 7.0, and 7.5. The colour range used in these maps goes from red to green, where red represents the most dangerous zones with an FS_L lower than 0.50 and green represents the

least susceptible to liquefaction with an FS_L greater than 10. The distribution maps were prepared by gradually changing the colour according to the obtained value of the FS_L range. These values have been classified into eight different categories: (i) $FS_L < 0.5$, (ii) $0.5 < FS_L < 0.75$, (iii) $0.75 < FS_L < 1.0$, (iv) $1.0 < FS_L < 1.3$, (v) $1.3 < FS_L < 1.5$, (vi) $1.5 < FS_L < 5.0$, (vii) $5.0 < FS_L < 10.0$, and (viii) $FS_L > 10.0$. The FS_L reveals the stability of the soil against liquefaction, with higher values indicating greater resistance. The maps prepared using the Tokimatsu and Yoshimi (1983) method appear much greener, indicating a higher FS_L , compared to those prepared using the IS 1893 (Part 1): 2016 method. This suggests that the Tokimatsu and Yoshimi method predicts higher FS_L values than the IS 1893 (Part 1): 2016 method. The maps also identify highly vulnerable districts for liquefaction susceptibility, such as Sitamarhi, Madhubani, and Supaul. These districts show high susceptibility even at a moderate range of $M_w = 6.0$, making them particularly concerning in terms of potential liquefaction-induced damage. For $M_w = 7.5$, the entire Bihar, except for a small region in Sasaram district, has an FS_L value lower than one ($FS_L < 1$). The liquefaction susceptibility of soil below the ground surface is greatly influenced by its depth. At the shallow depth, almost the entire Bihar is shown in red, but as the depth is prolonged, the redness goes greener. This means that Bihar is susceptible to liquefaction at shallower depths. However, northern Bihar is susceptible to liquefaction at higher depths as well.

5. Discussion

The geographical and topographical conditions of Bihar make it prone to multiple natural and man-made threats. Earthquakes, floods, droughts, fire outbreaks, and cyclones are among the various disasters that Bihar experiences. Numerous rivers that drain the Bihar plain accumulate alluvial deposits, which intensify the soil's potential to liquefy during earthquakes. Subsurface fault lines that penetrate from the Himalayan tectonic plate into the Gangetic Plains increase its vulnerability to earthquakes.

The ongoing investigation focuses on subsurface investigations in Bihar, India, which encompasses all 38 districts within the state. The results illustrated the relative variations among different parameters. It shows that the FS_L is significantly influenced by M_w , depth below ground surface, FC, and SPT N-value. As the value of M_w increases, the resistance against liquefaction decreases. It means that the soil is more susceptible to liquefaction at higher M_w . FS_L

increases with the increase in depth of soil below ground surface and SPT N-value. At a constant SPT N-value, liquefaction resistance increases with increased FC. Also, the deeper soil layers show higher stability against liquefaction than the shallower layers. This is an important consideration for construction projects and infrastructure development in the region.

The present study proposes that soil deposits at various locations in Bihar should be considered safe if their FS_L value is greater than 1.5 ($FS_L > 1.5$). It can be noted here that for the same set of data, the Tokimatsu and Yoshimi (1983) method shows a reduced likelihood of liquefaction susceptibility. To safeguard against seismic soil liquefaction, FS_L values determined from both methods should be in the safe range. Due to this, the method described in IS 1893 (Part 1): 2016 can be treated as an effective technique.

The past seismic data shows that the state is susceptible to moderate to severe magnitude earthquakes. At the moderate range of M_w , northern Bihar is susceptible to liquefaction, but at the higher range of M_w , almost the entire state is prone to liquefaction. This finding underscores the importance of considering M_w when assessing liquefaction hazards in the region. As Bihar is the most densely populated Indian state with poor construction

techniques and maintenance, the associated damage to properties and lives will be on a large scale.

The study reveals that the soil of Bihar is at high risk of liquefaction, highlighting the need for careful engineering and construction practices to mitigate seismic hazards effectively. The hazard zonation maps presented in this paper provide the liquefaction susceptibility microzonation of the state. Depending on the severity of the region, an appropriate design methodology can be adopted to safeguard against future liquefaction hazards. The outcome of this research is helpful to the local government as well as infrastructure development. A preventive technique to mitigate liquefaction may be employed during the construction phase.

5.1 Limitation

Bihar is the most densely populated Indian state, with moderate to severe incidents of earthquakes. Therefore, the damages are on a large scale. The scope of the current research is limited to the assessment of the liquefaction susceptibility of soil in this region. Attempts have been made to explore the entire state. For this purpose, one representative borehole from each of the 38 districts was selected.

A complete list of abbreviations is listed in *Appendix I*.

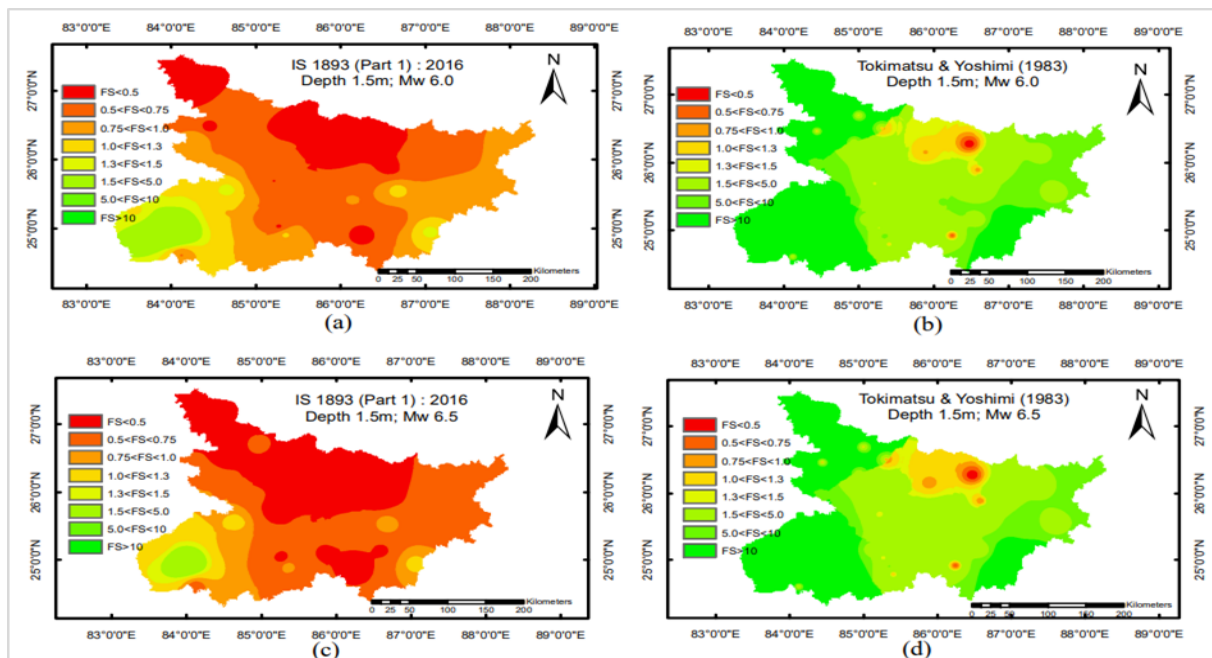


Figure 12 Hazard zonation map at 1.5m depth beneath ground surface according to IS 1893 (Part 1): 2016- (a) $M_w = 6.0$, (c) $M_w = 6.5$, and Tokimatsu and Yoshimi (1983)- (b) $M_w = 6.0$, (d) $M_w = 6.5$

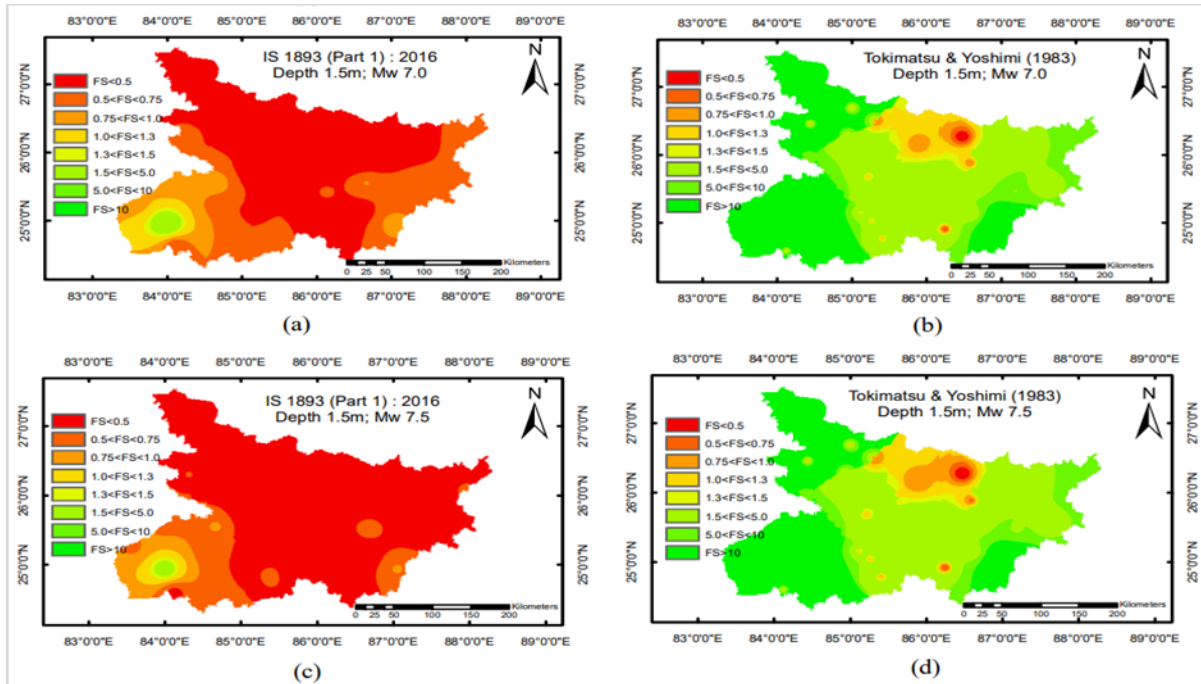


Figure 13 Hazard zonation map at 1.5m depth beneath ground surface according to IS 1893 (Part 1): 2016- (a) $M_w = 7.0$, (c) $M_w = 7.5$, and Tokimatsu and Yoshimi (1983)- (b) $M_w = 7.0$, (d) $M_w = 7.5$

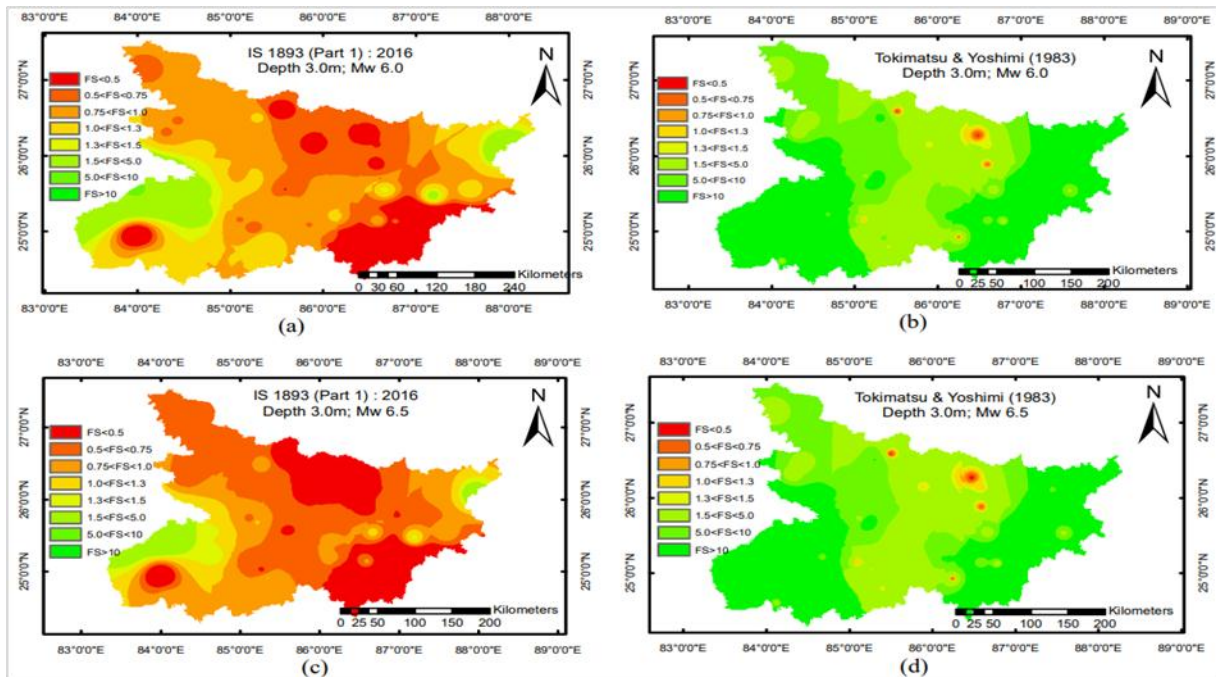


Figure 14 Hazard zonation map at 3.0m depth beneath ground surface according to IS 1893 (Part 1): 2016- (a) $M_w = 6.0$, (c) $M_w = 6.5$, and Tokimatsu and Yoshimi (1983)- (b) $M_w = 6.0$, (d) $M_w = 6.5$

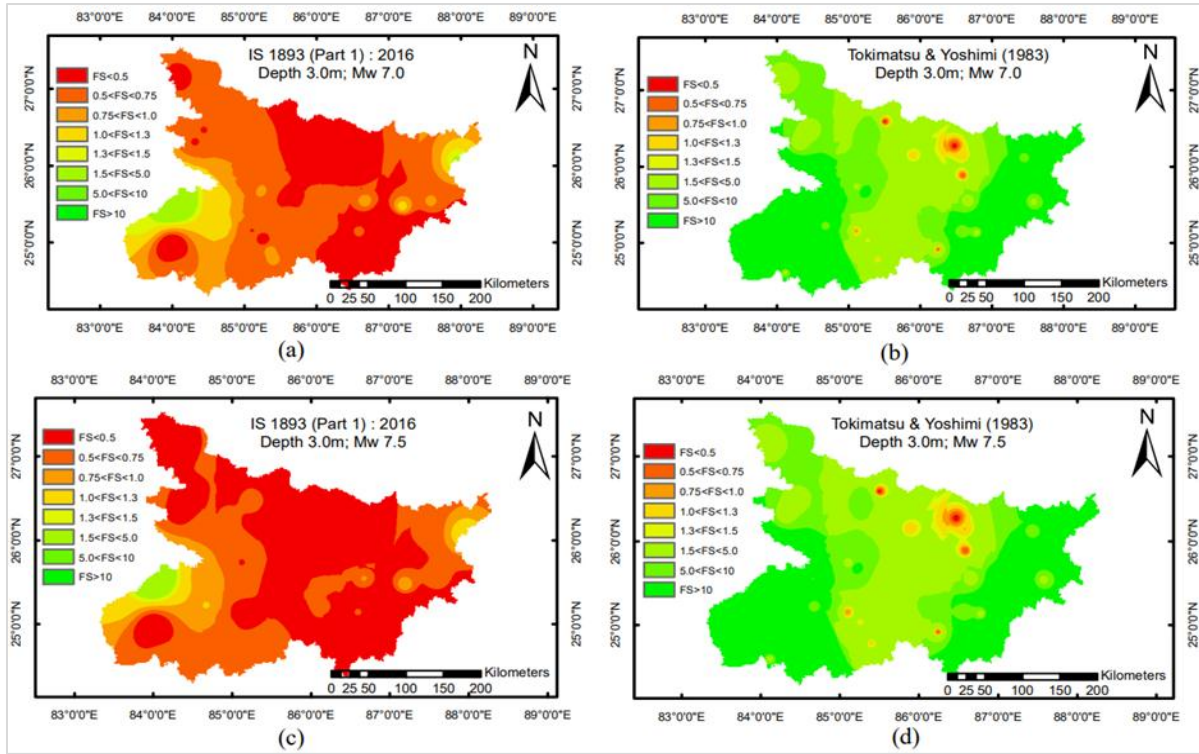


Figure 15 Hazard zonation map at 3.0m depth beneath ground surface according to IS 1893 (Part 1): 2016- (a) $M_w = 7.0$, (c) $M_w = 7.5$, and Tokimatsu and Yoshimi (1983)- (b) $M_w = 7.0$, (d) $M_w = 7.5$

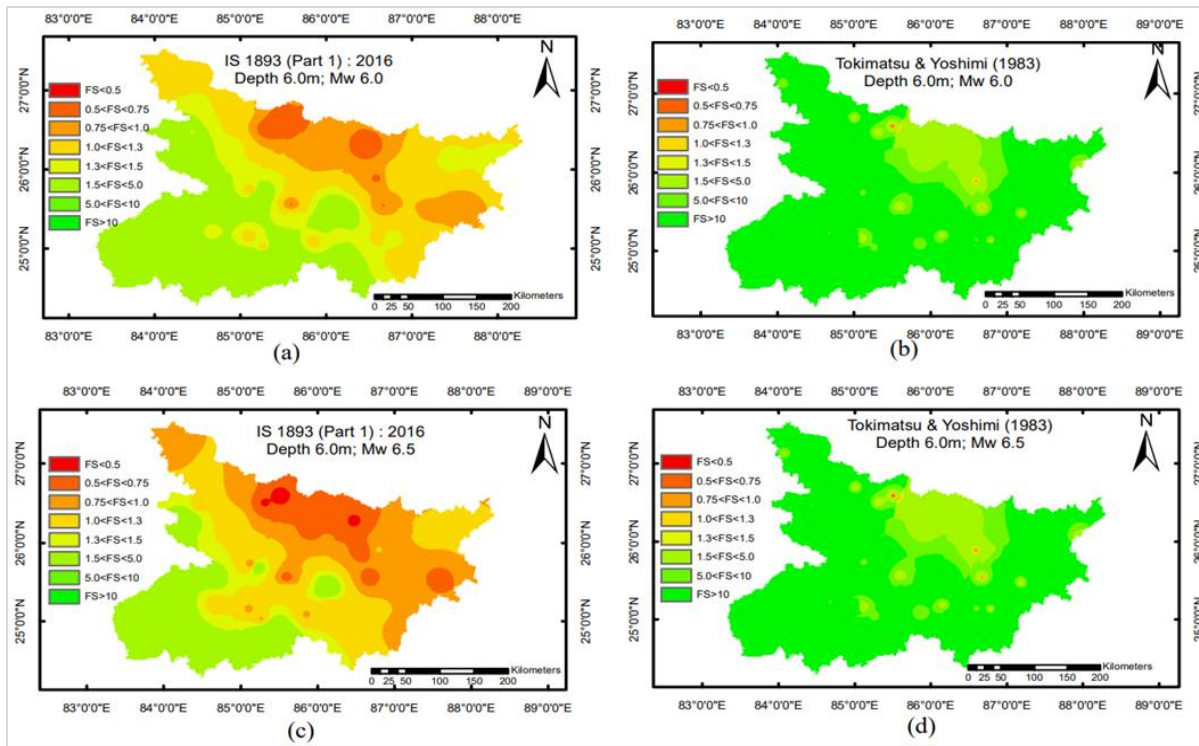


Figure 16 Hazard zonation map at 6.0m depth beneath ground surface according to IS 1893 (Part 1): 2016- (a) $M_w = 6.0$, (c) $M_w = 6.5$, and Tokimatsu and Yoshimi (1983)- (b) $M_w = 6.0$, (d) $M_w = 6.5$

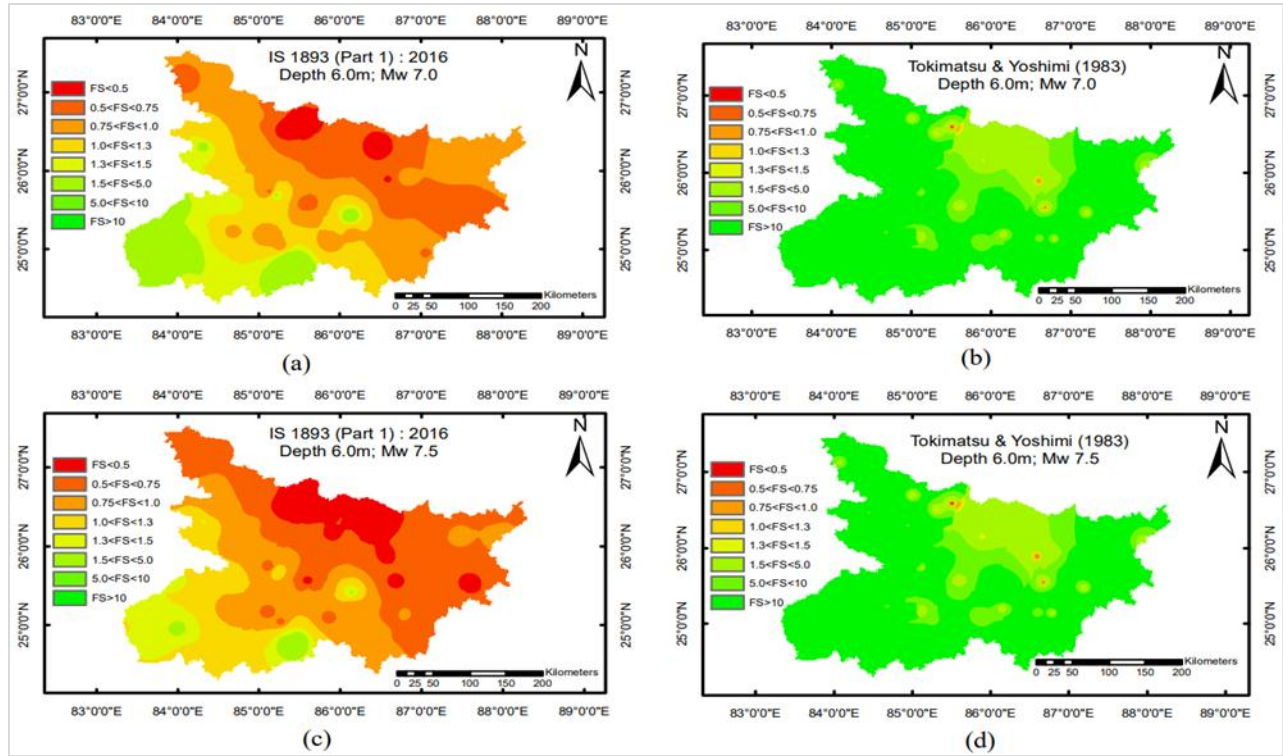


Figure 17 Hazard zonation map at 6.0m depth beneath ground surface according to IS 1893 (Part 1): 2016- (a) $M_w = 7.0$, (c) $M_w = 7.5$, and Tokimatsu and Yoshimi (1983)- (b) $M_w = 7.0$, (d) $M_w = 7.5$

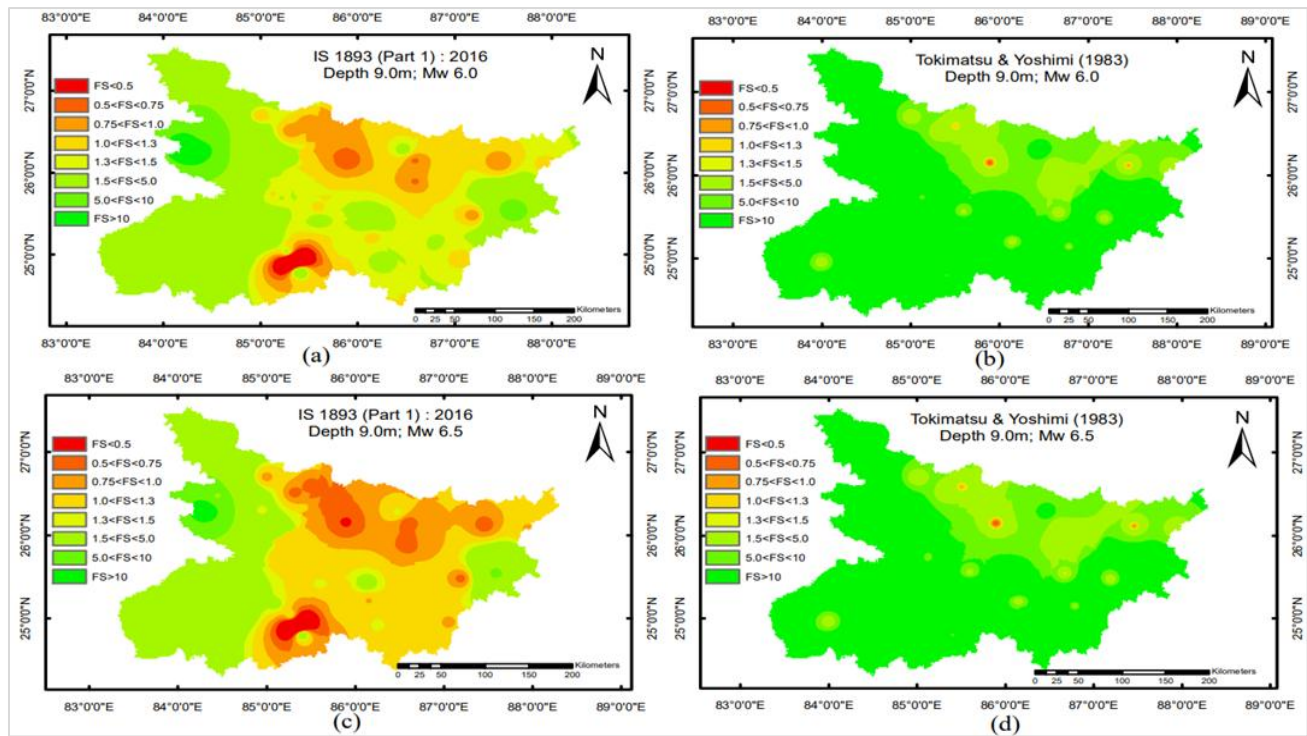


Figure 18 Hazard zonation map at 9.0m depth beneath ground surface according to IS 1893 (Part 1): 2016- (a) $M_w = 6.0$, (c) $M_w = 6.5$, and Tokimatsu and Yoshimi (1983)- (b) $M_w = 6.0$, (d) $M_w = 6.5$

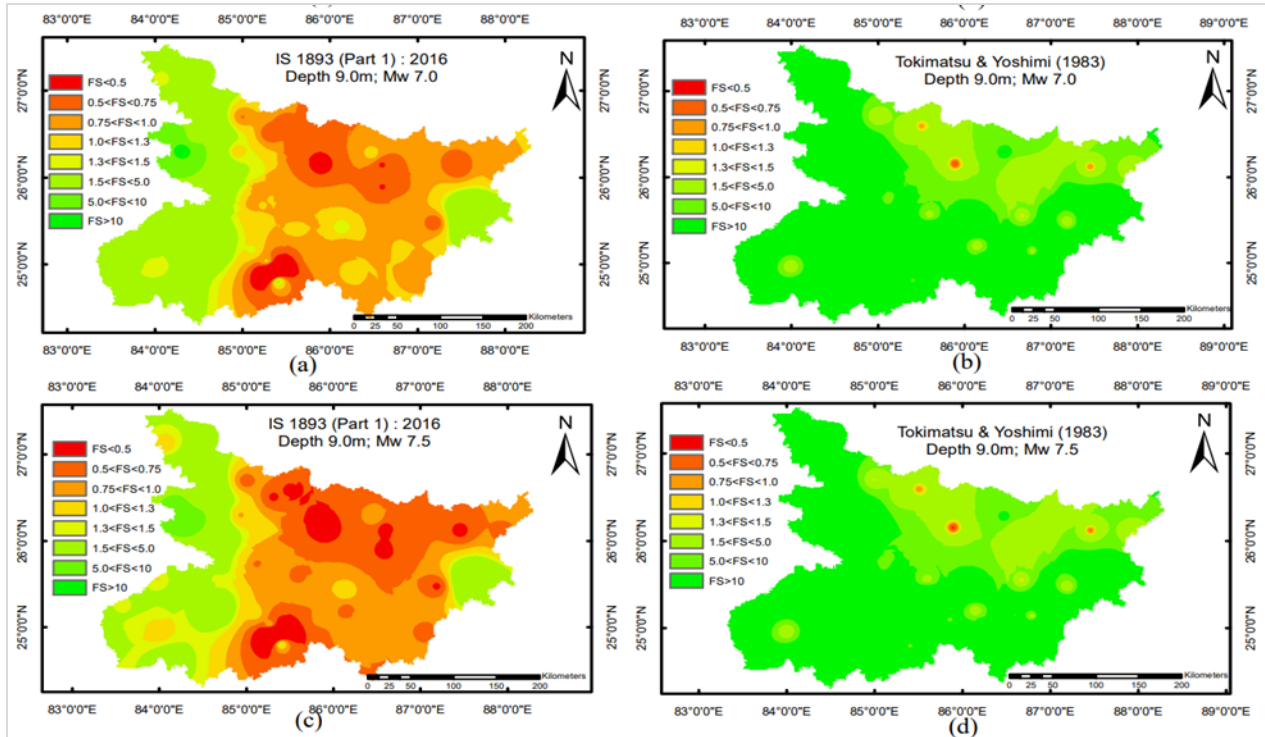


Figure 19 Hazard zonation map at 9.0m depth beneath ground surface according to IS 1893 (Part 1): 2016- (a) $M_w = 7.0$, (c) $M_w = 7.5$, and Tokimatsu and Yoshimi (1983)- (b) $M_w = 7.0$, (d) $M_w = 7.5$

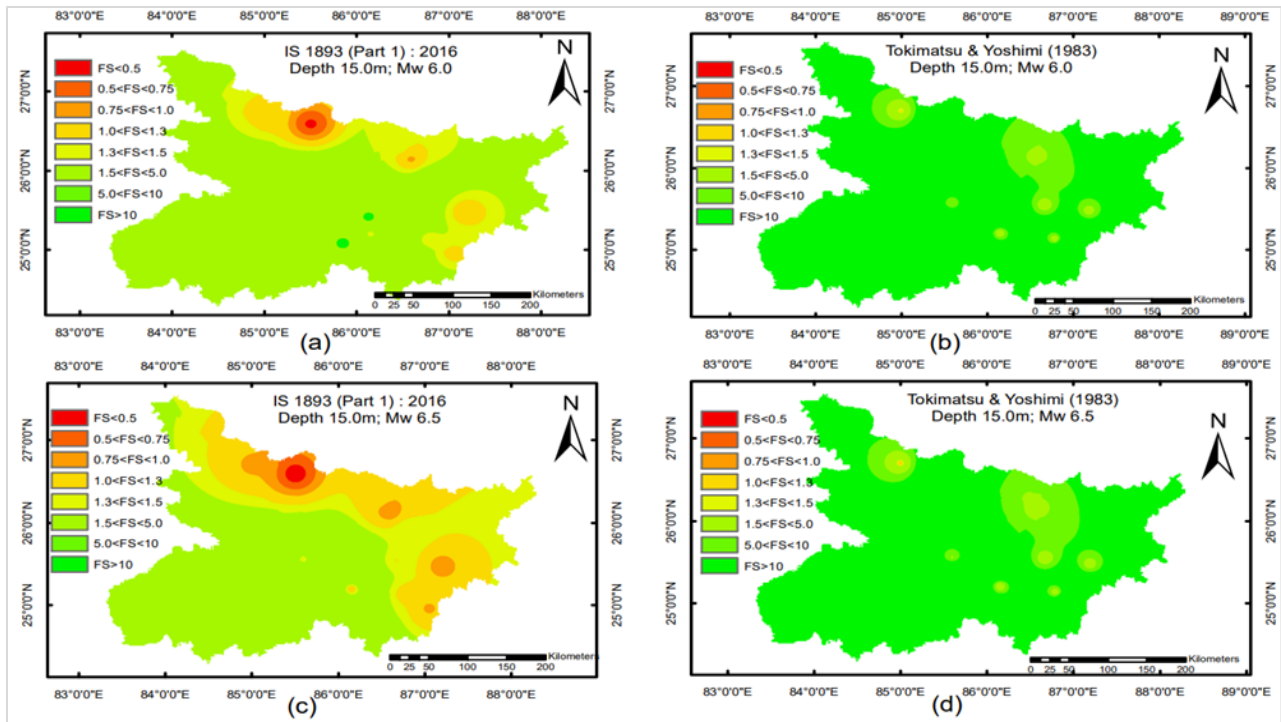


Figure 20 Hazard zonation map at 15.0m depth beneath ground surface according to IS 1893 (Part 1): 2016- (a) $M_w = 6.0$, (c) $M_w = 6.5$, and Tokimatsu and Yoshimi (1983)- (b) $M_w = 6.0$, (d) $M_w = 6.5$

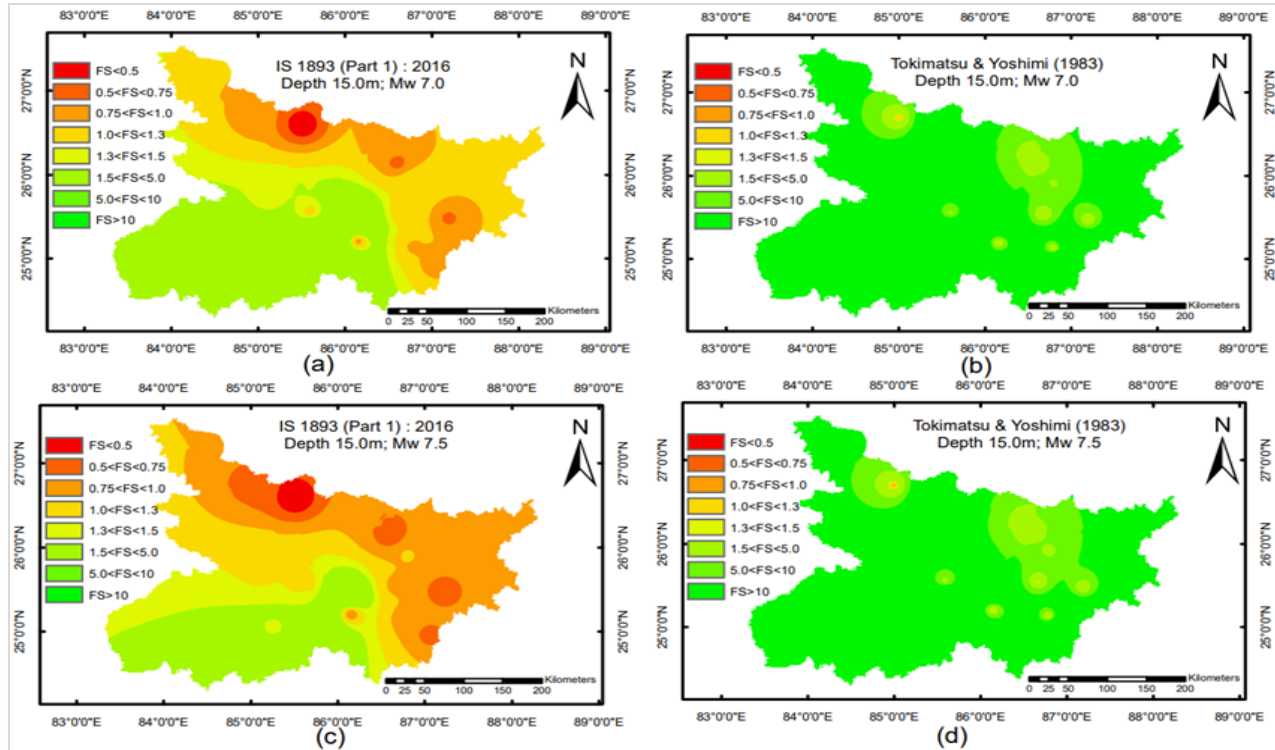


Figure 21 Hazard zonation map at 15.0m depth beneath ground surface according to IS 1893 (Part 1): 2016- (a) $M_w = 7.0$, (c) $M_w = 7.5$, and Tokimatsu and Yoshimi (1983)- (b) $M_w = 7.0$, (d) $M_w = 7.5$

6. Conclusion and future work

This study provides a comprehensive analysis of liquefaction susceptibility in the Bihar region, encompassing all 38 districts. Through a detailed examination of various parameters and methodologies, valuable insights have been obtained regarding the potential for soil liquefaction during seismic events. This highlights the significance of influencing factors.

The liquefaction of soil is significantly influenced by the depth of soil below the ground surface, M_w , SPT N-value, and FC. The liquefaction susceptibility of soil is determined by the combination of FC and SPT N-value. As per IS 1893 (Part 1): 2016 soil shows more resistance against liquefaction for FC below 10%, between 10% and 20%, and more than 20% if normalized SPT N-values are higher than 30, 25, and 20, respectively. The Tokimatsu and Yoshimi (1983) method shows that the soil is non-liquefiable for FC below 10% and above 10% if the normalized SPT N-value is greater than 25 and 15, respectively. Also, at the constant SPT N-value, the liquefaction resistance increases with an increase in the FC value of the soil. Liquefaction resistance increases with increasing soil depth. This indicates that the soil is more liquefiable

at shallow depths. The report shows that the Tokimatsu and Yoshimi (1983) method yields a higher FS_L value than that of the IS 1893 (Part 1): 2016 method.

The hazard zonation maps for Bihar reveal important insights into the liquefaction susceptibility of the soil in Bihar. Soil resistance against liquefaction improves with depth but diminishes with increasing earthquake magnitude. Regions like Sitamarhi, Madhubani, and Supaul districts are highly vulnerable, even at a moderate $M_w = 6.0$. Additionally, the northern districts of Bihar are more susceptible to liquefaction. For an earthquake magnitude of $M_w = 7.5$, except for a small region in Sasaram district, the entire state has an FS_L value below one, suggesting potential liquefaction risks. To ensure safety, the study suggests a minimum threshold value of 1.5 for the FS_L .

The current study reveals that the soil of Bihar is at high risk of liquefaction and could experience significant instability. These findings indicate the need for careful engineering and construction practices to mitigate seismic soil liquefaction hazards effectively in Bihar. Although the present research

tries to provide potential liquefaction zones in Bihar, further exploration and refinement of liquefaction susceptibility are required due to the heterogeneity of the soil.

Acknowledgment

None.

Conflicts of interest

The authors have no conflicts of interest to declare.

Data availability

Data considered in this study were gathered from a diverse range of reputable sources. These sources include the soil investigation report of the important infrastructure project of the Government of Bihar. It can be obtained from the different constructional departments of the Government of Bihar as well as from the laboratory of NIT Patna on reasonable request. A few of the soil test reports are publicly accessible at https://www.bseidc.in/soil_test_reports.php.

Author's contribution statement

Ishwar Chandra Thakur: Conceptualization, data collection, analysis, interpretation of result, validation, and writing- original draft. **Lal Bahadur Roy:** Study conception, supervision, writing- review and editing.

References

- [1] <https://censusindia.gov.in/census.website/data/atlas>. Accessed 8 January 2024.
- [2] http://bsdma.org/Welcoming_note.aspx. Accessed 8 January 2024.
- [3] Singh SK, Pandey AC. Geomorphology and the controls of geohydrology on waterlogging in Gangetic Plains, North Bihar, India. *Environmental Earth Sciences*. 2014; 71:1561-79.
- [4] Standard I. Criteria for earthquake resistant design of structures. Bureau of Indian Standards, Part. 1893.
- [5] Rajendran CP, John B, Rajendran K, Sanwal J. Liquefaction record of the great 1934 earthquake predecessors from the north Bihar alluvial plains of India. *Journal of Seismology*. 2016; 20:733-45.
- [6] Banerji S, Roy S, Wadia D, West W, Normand C, Banerji A, et al. The north Bihar earthquake, 1934. *Current Science*. 1935; 3(8):372-5.
- [7] Jain SK. Earthquake engineering: problems and prospects. *Indian Concrete Journal*. 1994; 68(11):605-6.
- [8] Jain SK. Earthquake safety in India: achievements, challenges and opportunities. *Bulletin of Earthquake Engineering*. 2016; 14:1337-436.
- [9] Gupta HK. Major and great earthquakes in the Himalayan region: an overview. *Earthquake Hazard and Seismic Risk Reduction*. 2000:79-85.
- [10] Sukhija BS, Rao MN, Reddy DV, Nagabhushanam P, Kumar D, Lakshmi BV, et al. Palaeoliquefaction evidence of prehistoric large/great earthquakes in north Bihar, India. *Current Science*. 2002:1019-25.
- [11] Singh CS, Anima K, Kumar B, Gautam E, Kumari EA. Environmental challenge due to climate change in Bihar, developing state of India. *Journal of Natural Sciences Research*. 2014; 4(13):21-8.
- [12] Raghucharan MC, Somala SN. Seismic damage and loss estimation for central Indo-Gangetic Plains, India. *Natural Hazards*. 2018; 94:883-904.
- [13] Burnwal ML, Burman A, Samui P, Maity D. Deterministic strong ground motion study for the Sitamarhi area near Bihar-Nepal region. *Natural Hazards*. 2017; 87:237-54.
- [14] Burman A, Gautam R, Maity D. DSHA based estimation of peak ground acceleration for Madhubani and Supaul districts near Bihar-Nepal Region. *Geotechnical and Geological Engineering*. 2020; 38:1255-75.
- [15] Shams R, Agrawal M, Gupta RK. Probabilistic seismic hazard assessment of Kishanganj, Bihar, India. *Journal of Earth System Science*. 2022; 131(4):257.
- [16] Dey S. A devastating disaster: a case study of Nepal earthquake and its impact on human beings. *IOSR Journal of Humanities and Social Science*. 2015; 20:28-34.
- [17] Rai DC, Singhal V, Raj SB, Sagar SL. Reconnaissance of the effects of the M7.8 Gorkha (Nepal) earthquake of April 25, 2015. *Geomatics, Natural Hazards and Risk*. 2016; 7(1):1-7.
- [18] Sinha AK. Seismic vulnerability assessment of buildings of Patna by rapid visual screening. *International Journal of Advanced Technology and Engineering Exploration*. 2022; 9(86):61-71.
- [19] Sinha AK. Rapid visual screening vulnerability assessment method of buildings: a review. *International Journal of Advanced Technology and Engineering Exploration*. 2022; 9(88):326-36.
- [20] Jain SK. Indian earthquakes: an overview. *Indian Concrete Journal*. 1998; 72:555-62.
- [21] Jain SK, Agrawal AK, Tripathi RP. Geotechnical damage due to Bihar earthquake of August 1988. In 2nd international conference on recent advances in geotechnical earthquake engineering and soil dynamics 1991 (pp. 1-7). University of Missouri—Rolla.
- [22] Marcussen E. Town planning after the 1934 Bihar-Nepal Earthquake: earthquake-safety, colonial improvements and the restructuring of urban space in Bihar. *Studies in Nepali History and Society*. 2017; 22(2):321-54.
- [23] Ranjith A, Kiran BM, Sanjith J, CL MK, Shwetha KG. Performance based seismic analysis of RC structural system under earthquake excitation. *International Journal of Advanced Technology and Engineering Exploration*. 2022; 9(91):735-58.
- [24] Usman F, Murakami K, Kurniawan EB. Disaster mitigation preparedness of Semeru volcano eruption. *International Journal of Advanced Technology and Engineering Exploration*. 2023; 10(108):1524-36.
- [25] Tang XW, Hu JL, Qiu JN. Identifying significant influence factors of seismic soil liquefaction and

- analyzing their structural relationship. *KSCE Journal of Civil Engineering*. 2016; 20:2655-63.
- [26] Hu J, Tan Y, Zou W. Key factors influencing earthquake-induced liquefaction and their direct and mediation effects. *Plos One*. 2021; 16(2):e0246387.
- [27] Konstantaras A, Petrakis NS, Frantzeskakis T, Markoulakis E, Kabassi K, Vardiambasis IO, et al. Deep learning neural network seismic big-data analysis of earthquake correlations in distinct seismic regions. *International Journal of Advanced Technology and Engineering Exploration*. 2021; 8(84):1410-23.
- [28] Reshma TV, Patnaikuni CK, Manjunatha M, Bharath A, Tangadagi RB. Influence of alccofine and polypropylene fibers on stabilization of soil—an investigational study. *International Journal of Advanced Technology and Engineering Exploration*. 2022; 9(89):551-62.
- [29] Thakur IC, Roy LB. Soil liquefaction potential in different seismic zones of Bihar, India. *Engineering, Technology & Applied Science Research*. 2022; 12(6):9471-6.
- [30] Gautam D, De MFS, Fabbrocino G. Soil liquefaction in Kathmandu valley due to 25 April 2015 Gorkha, Nepal earthquake. *Soil Dynamics and Earthquake Engineering*. 2017; 97:37-47.
- [31] Saxena S, Roy LB, Gupta PK, Kumar V, Paramasivam P. Model tests on ordinary and geosynthetic encased stone columns with recycled aggregates as filler material. *International Journal of Geo-Engineering*. 2024; 15(1):1-3.
- [32] Saxena S, Roy LB. The effect of geometric parameters on the strength of stone columns. *Engineering, Technology & Applied Science Research*. 2022; 12(4):9028-33.
- [33] Saxena S, Roy LB. Suitability analysis of stone column materials with PLAXIS. *Engineering, Technology & Applied Science Research*. 2022; 12(2):8421-5.
- [34] Cetin KO, Seed RB, Der KA, Tokimatsu K, Harder JLF, Kayen RE, et al. Standard penetration test-based probabilistic and deterministic assessment of seismic soil liquefaction potential. *Journal of Geotechnical and Geoenvironmental Engineering*. 2004; 130(12):1314-40.
- [35] Tokimatsu K, Yoshimi Y. Empirical correlation of soil liquefaction based on SPT N-value and fines content. *Soils and Foundations*. 1983; 23(4):56-74.
- [36] Seed HB, Idriss IM. Simplified procedure for evaluating soil liquefaction potential. *Journal of the Soil Mechanics and Foundations Division*. 1971; 97(9):1249-73.
- [37] Youd TL, Idriss IM. Liquefaction resistance of soils: summary report from the 1996 NCEER and 1998 NCEER/NSF workshops on evaluation of liquefaction resistance of soils. *Journal of Geotechnical and Geoenvironmental Engineering*. 2001; 127(4):297-313.
- [38] Putti SP, Satyam N. Ground response analysis and liquefaction hazard assessment for Vishakhapatnam city. *Innovative Infrastructure Solutions*. 2018; 3:1-4.
- [39] Chanda S, Kumar M, Kumar N, Shukla RP. Study of liquefaction potential at Jaigarh port using standard penetration test data and consequences: a case study. In *symposium in earthquake engineering 2022* (pp. 171-83). Singapore: Springer Nature Singapore.
- [40] Poddar P, Ojha S, Gupta MK. Probabilistic and deterministic-based approach for liquefaction potential assessment of layered soil. *Natural Hazards*. 2023; 118(2):993-1012.
- [41] Ghani S, Kumari S. Liquefaction susceptibility of high seismic region of Bihar considering fine content. In *basics of computational geophysics 2021* (pp. 105-20). Elsevier.
- [42] Mittal RK, Mahalakshmi N, Singh S. Evaluation of liquefaction screening criterion based on standard penetration test values. In *structures congress 2013: bridging your passion with your profession 2013* (pp. 2983-8). ASCE.
- [43] Satyam DN, Rao KS. Liquefaction hazard assessment using SPT and VS for two cities in India. *Indian Geotechnical Journal*. 2014; 44:468-79.
- [44] Bhattacharya P, Mukherjee SP, Das B. Prediction of liquefaction potential for Kolkata region by semi-empirical method. In *5th international conference on recent advances in geotechnical earthquake engineering and soil dynamics 2010* (pp. 1-8). Missouri University of Science and Technology.
- [45] Andrus RD, Stokoe IIKH. Liquefaction resistance of soils from shear-wave velocity. *Journal of Geotechnical and Geoenvironmental Engineering*. 2000; 126(11):1015-25.
- [46] Gurung L, Chatterjee K. Evaluation of liquefaction potential of Kolkata City, India: a deterministic approach. *Pure and Applied Geophysics*. 2023; 180(1):439-74.
- [47] Boulanger RW, Idriss IM. CPT and SPT based liquefaction triggering procedures. Report No. UCD/CGM.-14. 2014; 1:134.
- [48] Kumar S, Muley P, Syed NM. Soil liquefaction potential of Kalyani region, India. *Indian Geotechnical Journal*. 2023; 53(1):139-53.
- [49] Naik SP, Patra NR. Generation of liquefaction potential map for Kanpur city and Allahabad city of northern India: an attempt for liquefaction hazard assessment. *Geotechnical and Geological Engineering*. 2018; 36:293-305.
- [50] Muley P, Maheshwari BK, Paul DK. Liquefaction potential of Roorkee region using field and laboratory tests. *International Journal of Geosynthetics and Ground Engineering*. 2015; 1:1-3.
- [51] Bolton SH, Tokimatsu K, Harder LF, Chung RM. Influence of SPT procedures in soil liquefaction resistance evaluations. *Journal of Geotechnical Engineering*. 1985; 111(12):1425-45.
- [52] Bardet JP, Ichii K, Lin CH. EERA: a computer program for equivalent-linear earthquake site response analyses of layered soil deposits. University of

- Southern California, Department of Civil Engineering; 2000.
- [53] Muley P, Maheshwari BK, Kirar B. Liquefaction potential of sites in Roorkee region using SPT-based methods. *International Journal of Geosynthetics and Ground Engineering*. 2022; 8(2):26.
- [54] Dwivedi VK, Dubey RK, Thockhom S, Pancholi V, Chopra S, Rastogi BK. Assessment of liquefaction potential of soil in Ahmedabad Region, Western India. *The Journal of Indian Geophysical Union*. 2017; 21(2):116-23.
- [55] Jha S, Roshan AD, Pisharady AS, Bishnoi LR. A review of state of art for SPT based liquefaction hazard assessment. *Conference on structural mechanics in reactor technology 2017* (pp.1-10).
- [56] Hore R, Chakraborty S, Arefin MR, Ansary MA. CPT & SPT tests in assessing liquefaction potential. *Geotechnical Engineering* (00465828). 2020; 51(4).
- [57] Patriaman F, Fathani TF, Wilopo W. Liquefaction potential analysis in Palu Bay area. In *IOP conference series: earth and environmental science 2021* (pp. 1-12). IOP Publishing.
- [58] Wadi D, Wu W, Malik I, Ahmed HA, Makki A. Assessment of liquefaction potential of soil based on standard penetration test for the upper Benue region in Nigeria. *Environmental Earth Sciences*. 2021; 80:1-11.
- [59] Nilay N, Chakraborty P, Popescu R. Liquefaction hazard mapping using various types of field test data. *Indian Geotechnical Journal*. 2022; 52(2):280-300.
- [60] Ansari A, Zahoor F, Rao KS, Jain AK. Liquefaction hazard assessment in a seismically active region of Himalayas using geotechnical and geophysical investigations: a case study of the Jammu Region. *Bulletin of Engineering Geology and the Environment*. 2022; 81(9):1-19.
- [61] Ortiz-hernández E, Chunga K, Pastor JL, Toulkeridis T. Assessing susceptibility to soil liquefaction using the standard penetration test (SPT)—a case study from the city of Portoviejo, Coastal Ecuador. *Land*. 2022; 11(4):1-20.
- [62] Deviprasad BS, Chaitanya CK, Mazumder T, Vijaya R, Raja PS, Neeraj P, et al. Deterministic and probabilistic measures of liquefaction susceptibility: a comparison. *Indian Geotechnical Journal*. 2023; 53(1):208-19.
- [63] Standard B. Eurocode 8: design of structures for earthquake resistance. Part. 2005.
- [64] Shekhar S, Ram S, Burman A. Probabilistic analysis of piping in Habbit earthen embankment using monte carlo and subset simulation: a case study. *Indian Geotechnical Journal*. 2022; 52(4):907-26.
- [65] Acharya IP, Subedi M, KC R. Liquefaction hazard assessment of Kathmandu valley using deterministic and probabilistic approaches. In *Geo-Risk 2023* (pp. 307-17). ASCE.
- [66] Aytaş Z, Alpaslan N, Özçep F. Evaluation of liquefaction potential by standard penetration test and shear wave velocity methods: a case study. *Natural Hazards*. 2023; 118(3):2377-417.
- [67] Kundu P, Pain A, Das J. Earthquake-induced liquefaction potential and risk assessment of the world's largest mobile manufacturing plant, Noida, Uttar Pradesh. *Environmental Earth Sciences*. 2024; 83(7):194.
- [68] Hwang JH, Yang CW. Appraisal of SPT-N methods in liquefaction analysis by using the Chi-Chi earthquake data cases. *Sino Geotech*. 2003; 98:79-90.
- [69] Chang M, Kuo CP, Shau SH, Hsu RE. Comparison of SPT-N-based analysis methods in evaluation of liquefaction potential during the 1999 Chi-Chi earthquake in Taiwan. *Computers and Geotechnics*. 2011; 38(3):393-406.
- [70] Subasi DE, İkizler SB. Assessment of liquefaction potential of Erzincan province and its vicinity, Turkey. *Natural Hazards*. 2014; 73:1863-87.
- [71] Iwasaki T, Tokida K, Tatsuoka F. Soil liquefaction potential evaluation with use of the simplified procedure. In *1st international conference on recent advances in geotechnical earthquake engineering and soil dynamics 1981* (pp. 1-7). University of Missouri—Rolla.
- [72] Rahman MA, Ahmed S, Imam MO. Rational way of estimating liquefaction severity: an implication for Chattogram, the Port city of Bangladesh. *Geotechnical and Geological Engineering*. 2020; 38(2):2359-75.
- [73] Hossain MB, Roknuzzaman M, Rahman MM. Liquefaction potential evaluation by deterministic and probabilistic approaches. *Civil Engineering Journal*. 2022; 8(7):1459-81.
- [74] Mhaske SY, Choudhury D. GIS-based soil liquefaction susceptibility map of Mumbai city for earthquake events. *Journal of Applied Geophysics*. 2010; 70(3):216-25.
- [75] Anbazhagan P, Basavaraj S, Premalatha KV. Liquefaction hazard mapping of Chennai, India using SPT data. *International Journal of Earth Sciences and Engineering*. 2011; 4(2):223-32.
- [76] Ganapathy GP, Zaalishvili VB, Mel'kov DA, Dzeranov BV, Chandrasekaran SS. Mapping of soil liquefaction potential susceptibility for urban areas. *Geology and Geophysics of the South of Russia*. 2018(3):106-15.
- [77] Das S, Ghosh S, Kayal JR. Liquefaction potential of Agartala city in Northeast India using a GIS platform. *Bulletin of Engineering Geology and the Environment*. 2019; 78:2919-31.
- [78] Bhatt N, Pancholi V, Chopra S, Rout MM, Shah RD, Kothari GC. Rapid seismic hazard assessment of the Sabarmati river basin in Gujarat state, western India using GIS techniques. *Bulletin of Engineering Geology and the Environment*. 2019; 78:3927-42.
- [79] Satyanarayana RCN, Harika A. Study on liquefaction evaluation of subsoil strata along Visakhapatnam coastal area. In *Indian geotechnical conference 2021* (pp. 241-57). Singapore: Springer Nature Singapore.
- [80] Boumpoulis V, Depountis N, Pelekis P, Sabatakakis N. SPT and CPT application for liquefaction evaluation in Greece. *Arabian Journal of Geosciences*. 2021; 14:1-5.

- [81] Rawat A, Kumar D, Chatterjee RS, Kumar H. A GIS-based liquefaction susceptibility mapping utilising the morphotectonic analysis to highlight potential hazard zones in the East Ganga plain. *Environmental Earth Sciences*. 2022; 81(13):358.
- [82] Pancholi V, Bhatt N, Singh P, Chopra S. Multi-criteria approach using GIS for macro-level seismic hazard assessment of Kachchh rift basin, Gujarat, western India—first step towards earthquake disaster mitigation. *Journal of Earth System Science*. 2022; 131(1):3.
- [83] Ashikuzzaman M, Hossain A, Salan MS. Liquefaction assessment of Rajshahi city corporation, Bangladesh. *Indian Geotechnical Journal*. 2023; 53(2):455-64.
- [84] Seed HB, Idriss IM. Analysis of soil liquefaction: Niigata earthquake. *Journal of the Soil Mechanics and Foundations Division*. 1967; 93(3):83-108.
- [85] De APA, Chan CK, Seed HB. Sand liquefaction in large-scale simple shear tests. *Journal of the Geotechnical Engineering Division*. 1976; 102(9):909-27.



Ishwar Chandra Thakur is a Ph.D. research scholar at National Institute of Technology, Patna, Bihar, India and currently working as an Assistant Professor of Civil Engineering Department at Darbhanga College of Engineering, Darbhanga, under the Department of Science, Technology

and Technical Education (DSTTE), Govt. of Bihar, India. Before this, he worked as a Lecturer of the Civil Engineering Department at Government Polytechnic, West Champaran under the same department DSTTE for about 4 years (i.e. from 2018 to 2022). Altogether he has more than 5 years of teaching experience. He is also an Associate Member of the Institute of Engineers (India). He has received B.Tech (2011) and M. Tech (2016) from BIT Sindri, Dhanbad with distinction marks.

Email: ishwart.phd20.ce@nitp.ac.in



Dr. Lal Bahadur Roy is working as a Professor of Civil Engineering at National Institute of Technology Patna, Bihar, India since August 2013. Before this, he worked as an Associate Professor of Civil Engineering at NIT Patna for seven years (2006-2013), as an Associate Professor for 8.5 years (

i.e., from 1995 to 2001 and from 2002 to 2004), as a Dean Research and Consultancy for 3 years (i.e., from April-2019 to April-2022), and Head of Irrigation Engineering Department (4 years) at Arba Minch University in Ethiopia, as an Assistant Professor at Water and Land Management Institute, Patna for ten years (from 1988 to 1995, 2001 to 2002 and 2004 to 2006), as an Assistant Engineer for one year in Water Recourses Department Govt. Of Bihar (i.e., 1987-1988). He has altogether 35 years of experience in teaching, training, research, and academic administration. His specialization includes irrigation water management with a special focus on land drainage, soil stabilization, and

swelling clays. Dr. Roy has presented technical papers at a number of national and international seminars and conferences in India and other countries. Many national and international journal papers are to his credit. He also worked as a member of the Editorial Board of the Ethiopian Journal of Water Science and Technology during the period (1996-2004). He has also authored two books titled Application of Graphic in Engineering and Static Graphics respectively. His degrees are Ph.D. (1995) from Patna University, India, M.E Honr's (1987) from the University of Roorkee, India, and B.Sc Engg (with Distinction) from Ranchi University, India.
Email: lbroy@nitp.ac.in

Appendix I

S. No.	Abbreviation	Description
1	BIS	Bureau of Indian Standard
2	CRR	Cyclic Resistance Ratio
3	CRR _{7.5}	Cyclic Resistance Ratio for Earthquake Magnitude 7.5
4	CSR	Cyclic Stress Ratio
5	FC	Fines Content
6	FS _L or FS	Factor of Safety Against Liquefaction
7	GIS	Geographical Information System
8	MMI	Modified Mercalli Intensity
9	MSF	Magnitude Scaling Factor
10	M _w	Magnitude of earthquake
11	PGA	Peak Ground Acceleration
12	SPT	Standard Penetration Test